

International Atomic Energy Agency

INDC(CCP)-319/L

INDC

INTERNATIONAL NUCLEAR DATA COMMITTEE

TRANSLATION OF SELECTED PAPERS
PUBLISHED IN YADERNYE KONSTANTY (NUCLEAR CONSTANTS 3, 1986)

(Original Report in Russian was distributed
as INDC(CCP)-267/G)

Translated by the IAEA

September 1990

IAEA NUCLEAR DATA SECTION, WAGRAMERSTRASSE 5, A-1400 VIENNA

TRANSLATION OF SELECTED PAPERS
PUBLISHED IN YADERNYE KONSTANTY (NUCLEAR CONSTANTS 3, 1986)

(Original Report in Russian was distributed
as INDC(CCP)-267/G)

Translated by the IAEA

September 1990

Reproduced by the IAEA in Austria
September 1990

90-04597

Contents

Experimental and Evaluated Data on Secondary Neutron Spectra from Reactions on Iron, Chromium and Nickel Nuclei By S.P. Simakov	5
Evaluation of Neutron Cross-Sections for Iron Isotopes in the Resonance Region By V.G. Pronyaev, A.V. Ignatyuk	13
Scattering of 6 MeV Neutrons on Vanadium By A.V. Polyakov, G.N. Lovchikova, V.A. Vinogradov, B.V. Zhuravlev, O.A. Sal'nikov, S.Eh. Sukhikh	27
Inelastic Scattering of Neutrons on ^{93}Nb Nuclei By Yu.A. Nemilov, Ya.M. Kramarovskij, E.D. Teteren, L.P. Pobedonostsev	33
Integral Prompt Fission Neutron Spectrum from 1.5 MeV Neutron Induced Fission of ^{232}Th By S.Eh. Sukhikh, G.N. Lovchikova, V.A. Vinogradov, B.V. Zhuravlev, A.V. Polyakov, O.A. Sal'nikov	37
Measurement of the Radiative Neutron Capture Cross-Section for ^{238}U in the 4-460 keV Energy Region By L.E. Kazakov, V.N. Kononov, G.N. Manturov, E.D. Poletaev, M.V. Bokhovko, V.M. Timokhov, A.A. Voevodskij	45
Evaluation of Mean Resonance Parameters for ^{235}U , Plutonium Isotopes and ^{241}Am Using Data from the Resolved Resonance Region By V.A. Kon'shin, N.K. Salyakhov	61

EXPERIMENTAL AND EVALUATED DATA ON SECONDARY NEUTRON SPECTRA
FROM REACTIONS ON IRON, CHROMIUM AND NICKEL NUCLEI

S.P. Simakov

A knowledge of the cross-sections for the interaction of neutrons with iron, chromium and nickel nuclei as basic structural components of nuclear facilities is of great practical importance. In the neutron energy range of the order of a megaelectronvolt and above, the principal contribution to the total cross-section is made by the inelastic scattering process and the $(n,2n)$, (n,np) and $(n,n\alpha)$ reactions. From an applied point of view, substantial importance also attaches to a knowledge of the energy distributions of the secondary neutrons from these reactions, in accordance with which "softening" of the neutron spectrum occurs in the reactor. At present these physical quantities need to be known with an accuracy of 5-20% [1]. The present paper considers the qualitative adequacy of experimental and evaluated data for meeting this requirement.

The comparatively light nuclei of iron, chromium and nickel are characterized by the slight density of the low-lying nuclear levels, and therefore experimental data on inelastic interactions of neutrons with energies up to 5 MeV are usually presented in the form of partial inelastic scattering cross-sections with excitation of individual levels. We shall therefore remain in the higher energy region, in which it is possible experimentally to derive information on the continuous energy distributions of secondary neutrons.

Let us consider two libraries of evaluated neutron data for a natural mixture of chromium, iron and nickel isotopes, namely the fourth edition of the American library ENDF/B-IV [2], and the second edition of the Japanese library JENDL-2 [3]. Table 1 lists the experimental works (with the exception of those carried out for energies of 14-15 MeV) devoted to an investigation of the spectra of secondary neutrons formed as a result of the interaction of fast neutrons with the elements in question.

The fullest information is given for iron, while for the other elements it is limited to the results of only 2-3 studies. The experimental cross-sections (with the exception of study [4]) were measured by the time-of-flight method. These data usually agree with each other, and also with other data under conditions of coinciding energies and nuclei, which is an indication of their reliability.

Figure 1 shows the nuclear temperatures characterizing the energy dependence of the inelastic scattering spectra for iron, derived by various authors. As will be seen, the temperatures at neutron energies up to 10 MeV are in good agreement among themselves and with the evaluated data from the JENDL-2 library (the data spread at 14 MeV indicates the considerable divergence among the experimental spectra at this energy). The evaluated data for chromium and nickel nuclei are in poor agreement with the experimental figures (cf the results of study [8] in Fig. 2). As is apparent from this figure, the evaluated data from the ENDF/B-IV library, in which a "flow" representation is used, are likewise in unsatisfactory agreement with experiment.

Let us consider the experimental data derived at 14-15 MeV. The relatively large number of independent experiments at these energies permits the drawing of specific conclusions regarding the reliability of the various results. At an initial energy of 14 MeV, the channels for the (n,2n), (n,np) and (n,n α) reactions are open in the nuclei under consideration, in addition to the (n,n') reaction channel. Hence, the secondary neutron spectrum comprises the sum of the neutron spectra for all these reactions, i.e. the emission spectrum.

Table 2 lists the principal experimental investigations with an indication of various parameters. In the first group of experiments (the upper part of Table 2) we find those in which the time resolution of the neutron spectrometer, referred to its time base ($\Delta t/L$), was greater than 1 ns/m. In the experiments with such moderate resolution, the greatest

reliability attaches to the data on the low energy part of the emission spectrum, since in the high energy part substantial systematic errors are possible, associated with incorrect division of the elastically scattered neutron peak. As will be seen from Fig. 3, the results of these investigations, which were mostly carried out during the period 1966-1972, reveal significant discrepancies in the secondary neutron energy region $E' < 1$ MeV. An experiment mounted in 1979 with the specific aim of investigating the low energy part of the spectra [19] confirmed the data of study [12]. In the light of the methodological sophistication of these studies, it can be stated that for iron, chromium and nickel a complete picture of the low energy part of the emission spectra at 14 MeV can be derived on the basis of the data from Refs [12, 19].

In recent years, accompanying the improvement in the resolving power of neutron spectrometers, the attention of researchers was drawn to the high energy part of emission spectra. The relevant studies (at $\Delta t/L < 1$ ns/m) are listed in the second part of Table 2, and their results are also given in Fig. 3. As will be observed from the figure, there is a discrepancy between the data from the various studies, although it can be confidently asserted that, in the case of inelastic scattering of neutrons, collective states of the ^{56}Fe nucleus with spins 2^+ and 3^- are very probably excited. This conclusion is based on the fact that the position and value of the maxima in the high energy part of experimental spectra for inelastically scattered neutrons can be described in terms of a strong channel coupling model, assuming the collective nature of the lowest states of the ^{56}Fe nucleus (cf., e.g., Ref. [15]).

As regards evaluated data, as can be seen from Fig. 4 the neutron spectra in the ENDF/B-IV library describe the experimental data relatively well. In the case of chromium, it is necessary to make a correction for the intercalated spectra to the data of the ENDF/B-IV library.

A new type of experiment carried out by the correlation method (measurement of emitted neutrons for coincidences with γ quanta) (end of the 1970s) [24-26] provided unequivocal information on the neutron spectra from the $(n,n'\gamma)$ reaction, which gives an idea of the first and subsequent neutron spectra. The relevant works are listed in the third part of Table 2, and their results for the ^{56}Fe nucleus are given in Fig. 5.

The complexity of the correlation experiments is responsible for the divergence in the results of the different authors. However, a general trend, which can be discerned in all studies, lies in the fact that the neutron spectrum from the $(n,n'\gamma)$ reaction at $E' \leq E + Q_{n2n}$, when the emission channel of the second neutron from the excited ^{56}Fe nucleus opens, drops to zero. In principle this tendency is correctly reflected in the data of the ENDF/B-IV library, while data on the first neutron spectrum embodied in the JENDL-2 library do not reflect this trend. In the case of chromium and nickel nuclei, an incorrect representation is used in the ENDF/B-IV library for the first neutron spectrum. And although information on the Cr $(n,n'\gamma)$ and Ni $(n,n'\gamma)$ reactions is not available, nevertheless - as experimental data for neighbouring nuclei show [25] - the neutron spectra for the $(n,n'\gamma)$ reaction must have, for $E' \leq E + Q_{n2n}$, a dependence on E' which tends to zero. This circumstance should be taken into account when correcting the evaluated data files. On the basis of the present analysis the following conclusion may be drawn. For iron, there is now sufficient experimental material available to permit inferences regarding the structure of the neutron spectra in the 5-15 MeV neutron energy region. Regarding the evaluated data, we may note the satisfactory parameterization of the nuclear temperatures in the JENDL-2 library and of the first and second neutron spectra at 14 MeV in the ENDF/B-IV library. These positive factors should be taken into account when preparing a new edition of the evaluated data. Regarding experimental results for chromium and nickel, these are relatively few and the evaluated data are in poor agreement with them.

REFERENCES

1. WRENDA 83/84: Rep. INDC(SEC)-88/URSF. Vienna: IAEA, 1983.
2. ENDF/B Summary documentation: Rep. ENDF-201. Erocklaven, 1975.
3. Janakoshi H. J. Nucl. Sci. and Technol., 1980, v.17, p.477; Kikuchi Y. Ibid., p.567.
4. Ewing R.I., Fonger T.W. Bull. Amer. Phys. Soc., 1961, v.6, N 2, p.149.
5. Thomson D.E. Phys. Rev., 1963, v.129, N 4, p.1649.
6. Seth K.K., Wilensick R.M., Griffy T.A. Phys. Letters, 1964, v.11, p.308.
7. Maruyama M. Nucl. Phys., 1969, v.A131, p.145.
8. Birukov N.S., Zhuravlev B.V., Kormilov N.V. et al.. Yad. Fiz., 1974 Vol. 19, No. 6, p. 1190 (in Russian).
9. Linley W.E., Perey F.G. NES special publication, 1975, v.425, p.683.
10. Marcinkowski A., Pinley R.W., Randers-Jeherson G. e.a. Nucl. Sci. and Engng, 1983, v.63, p.13.
11. Schechtman R.M., Anderson J.D. Nucl. Phys., 1966, v.77, p.241.
12. Sal'nikov O.A., Lovchikova G.N., Kotel'nikova G.V. et al., Yad. Konst., 1971, No. 7, p. 134 (in Russian).
13. Fujita I., Sonoda M., Katase A. J. Nucl. Sci. and Technol., 1972, v.9, p.301.
14. Hermsdorf D., Meister A., Sassonoff S. e.a. Rep. ZFK-277. Dresden, 1974.
15. Lychagin A.A., Devkin B.V., Vinogradov V.A. et al., FEHl Preprint 1406, Obninsk, 1983 (in Russian).
16. Mathur S.C., Buchanan P.S., Morgan L.L. Phys. Rev., 1969, v.186, p.1038.
17. Clayeux G., Voignier J. Rep. CEA-R-4279. France, 1972.
18. Shin K., Baegava T., Hyodo T. Trans. Amer. Nucl. Soc., 1980, v.34, p.657.
19. Chalupka A., Vonach H., Wanninger F. Rep. ZFK-382. Dresden, 1979.
20. Hammerdiener J.L. Doctor Thesis. Livermore, 1972.
21. Takahashi A., Yamamoto J. Rep. A-83-01. Osaka, 1983.
22. Takahashi A., Fukazawa M., Yanagi J. Rep. A-83-08. Osaka, 1984.
23. Gul E., Anwar M., Ahmad M. e.a. Phys. Rev., 1985, v.C31, p.74.
24. Stengl G., Uhl K., Vonach H. Nucl. Phys., 1977, v. A290, p.109.
25. Kozyr' Yu.E., Prokopets G.A., Izv. AN SSSR. Ser. Fizich 1978, Vol. 42, p. 140 (in Russian).
26. Lychagin A.A., Devkin B.V., Vinogradov V.A. et al., FEHl Prepint 1722, Obninsk, 1985 (in Russian).

Paper received by editors on 24 December 1985.

Table 1. Nuclei and initial energies for which secondary neutron spectra were measured.

Nucleus	Initial energy, MeV	Literature reference
Iron	5; 7	[4]
"	7	[5]
"	6	[6]
Nickel	3,6-8,5	[7]
Iron,Chromium,Nickel	9,1	[8]
" " "	4-8,5	[9]
Iron	25,7	[10]

Table 2. Experimental investigations of secondary neutron spectra at 14-15 MeV.

Process measured, resolution	Element	$\Delta t/L$, ns/m	Angles, deg.	E' , MeV	Lit. ref.
$\Delta t/L > 1$ ns/m	Iron	1,6	30, 90, 120	1-5	[11]
	"	5,3	90	0,5-7	[16]
	Iron, chromium, nickel	3,5	31-151	0,1-14	[12]
	Iron, nickel	3,8	90	0,1-7	[17]
	Iron, chromium, nickel	2,5	110	2-6,5	[13]
	" " "	1,5	40-150	2-14	[14]
	Nickel	-	120	2,5-16	[18]
	Iron, chromium, nickel	2,5	Integral with respect to angles	0,3-6	[19]
$\Delta t/L < 1$ ns/m	Iron, nickel	0,2	45-135	1-14	[20]
	Iron	0,5	60	0,5-14	[15]
	Iron, chromium, nickel	0,2	15-143	0,6-14	[21]
	Iron	0,13	45	3-14	[22]
	"	0,9	30, 45, 60	1-14	[23]
Inelastic scattering	Iron	-	Integral with respect to angles	1-8,5	[24]
	"	-	70	0,6-4,1	[25]
	"	-	Integral with respect to angles	0,2-9	[26]

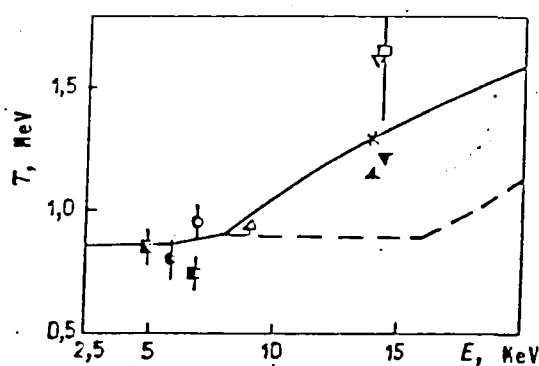


Fig. 1. Iron nucleus temperature as a function of incident neutron energy. Experimental data from studies: \square - [4]; \circ - [5]; \bullet - [6]; Δ - [8]; \times - [11]; \square - [12]; \blacktriangle - [13]; \blacktriangledown - [14]; ∇ - [15]. Evaluated data from the JENDL-2 library: ——— - nuclear temperature after emission of first neutron; - - - - the same for second neutron.

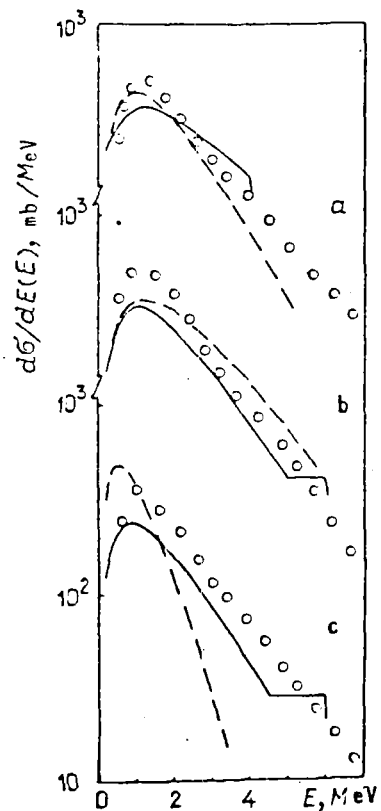


Fig. 2. Differential cross-sections for inelastic scattering of neutrons on nuclei of iron (a), chromium (b) and nickel (c) at an energy of 9.1 MeV (in this and subsequent figures the secondary neutron energy is laid off on the x-axis): o - experimental data from Ref. [8]; evaluated library data: ——— - ENDL/B-IV; - - - - JENDL-2.

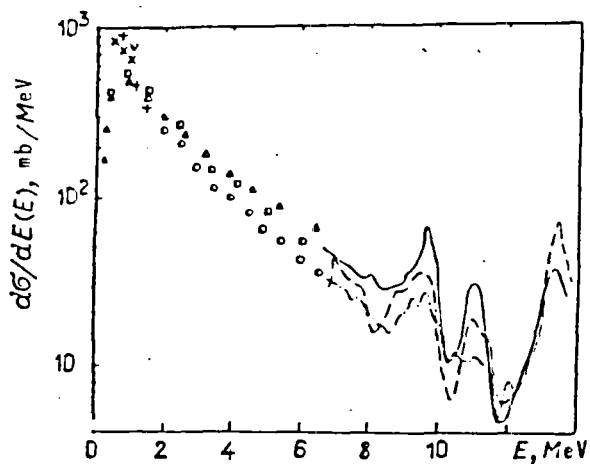


Fig. 3. Differential cross-sections for neutron emission by the (Fe + n) reaction at energy 14-15 MeV. Experimental data from studies: v - [11]; Δ - [12]; o - [14]; + - [16]; x - [17]; □ - [19]; ··· - [15]; - - - - [20]; ——— - [21].

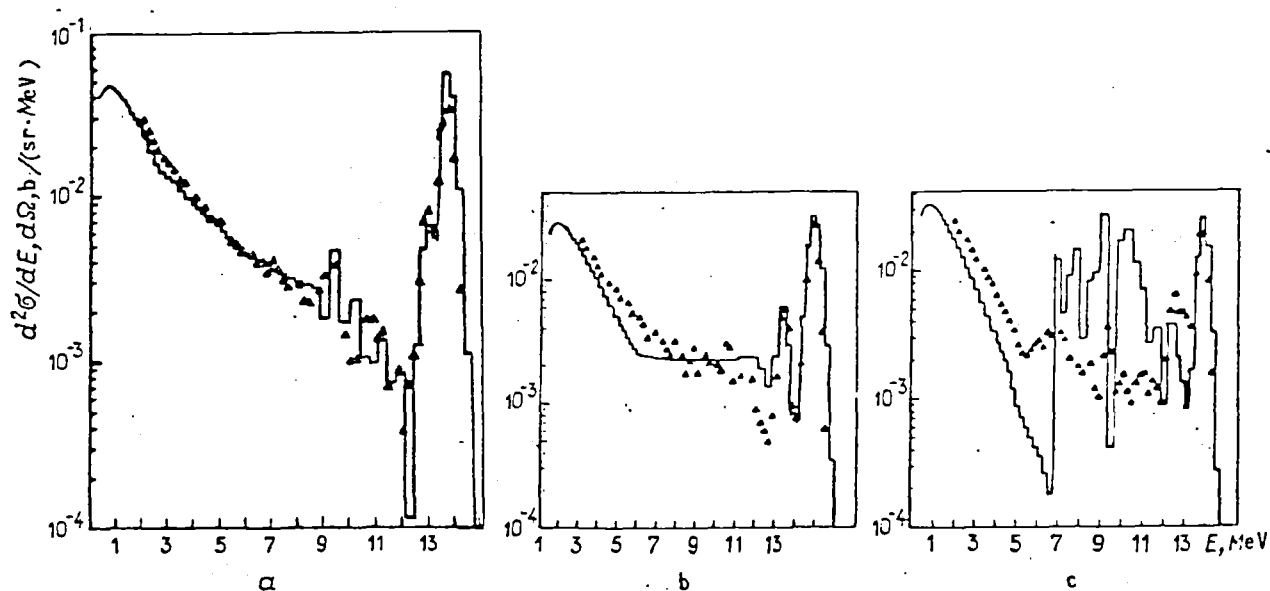


Fig. 4. Double differential cross-sections for neutron emission at initial energy 14 MeV for nuclei of iron (a), nickel (b) and chromium (c) at an angle of 80°. Data: \blacktriangle - experimental [21]; — - evaluated (ENDF/B-IV).

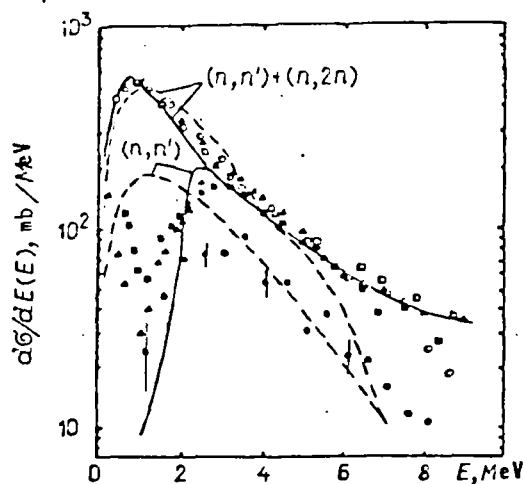


Fig. 5. Differential inelastic scattering cross-sections for the (n,n') reaction and emission [sum of (n,n') and $(n,2n)$ reaction cross-sections] at initial energy 14-15 MeV for the iron nucleus. Experimental data from studies: Δ - [15]; \circ - [19] (integrated in the range 0.5 MeV); \bullet - [24]; \square, \blacksquare - [25]; \blacktriangle - [26]. Evaluated data from libraries: — - ENDF/B-IV; - - - - JENDL-2.

EVALUATION OF NEUTRON CROSS-SECTIONS FOR IRON ISOTOPES
IN THE RESONANCE REGION

V.G. Pronyaev, A.V. Ignatyuk

Neutron cross-sections for the isotopes $^{54,57,58}\text{Fe}$ in the 10^{-5} eV-500 keV energy region and for ^{56}Fe in the 10^{-5} eV-850 keV energy region were evaluated. The evaluation (TsYaD-2) was based mainly on experimental data obtained since 1975. Particular attention was paid to the description of cross-section structure in a wide neutron energy range, which makes possible correct allowance for cross-section self-shielding when performing neutron-physical calculations of systems with a hard spectrum, containing iron.

At the present time users of evaluated neutron cross-sections have available files of data on iron from the ENDF/B-IV [1], TsYaD-1 [2], ENDL-82 [3] and JENDL-II [4] libraries of evaluated neutron cross-sections. In comparing cross-sections from various libraries averaged over broad groups [5], one must note the satisfactory agreement of total cross-sections and the substantial divergence in respect of capture cross-sections (Fig. 1,a,b). Thus, even ignoring the evaluation in the ENDL-82 library, which is systematically higher than the others, the divergence among the various groups in a 26-group representation lies within a range of 30-50% for the capture cross-section relating to a natural mixture of iron isotopes.

A shortcoming of all evaluated neutron cross-section files for iron and its isotopes is that the resolved resonance region is limited by a neutron energy of 200-300 keV, and above this level there occurs either a smoothing of the cross-sections or a region of unresolved resonances with average resonance parameter values. Here, allowance for self-shielding of the cross-sections calls for the introduction of supplementary cross-section fluctuation models, which do not give an unequivocal answer to the question regarding the value of the cross-section self-shielding coefficient in this region.

The performance recently of measurements of total cross-sections for the ^{56}Fe isotope up to an energy of 850 keV [6], together with the data from earlier studies, and also the results of measuring such characteristics as the area under the capture cross-section for individual resonances

$(A_{\gamma}^{\Gamma} = g_{n\gamma}^{\Gamma} \Gamma_{\gamma}^{\Gamma} / \Gamma_{\text{tot}}^{\Gamma})$, may serve as a basis for broadening the region of resolved resonances up to a higher energy. There are two basic factors preventing this broadening. Firstly, the upper boundary of this region for resonances with different spin characteristics can vary quite considerably; the format limitations of the ENDF-V library at present do not permit the formal introduction of another upper limit for states with different spins. The second limitation is associated with the number of resonances considered in deriving the "flow" representation with a particular pre-set accuracy. For contemporary computers this number should, it would appear, be limited by the 300-400 resonance level. However, by introducing "pseudo-isotopes" for each spin state it has proved possible - without any change in format and processing programs - to use various upper limits for sequences of levels with different orbital moments. S-wave resonances governing the global structure of the total cross-section and scattering cross-section are usually known up to a higher energy than p- and d-wave resonances, and hence by using the "pseudo-isotope" method it may be hoped that not only the mean cross-sections but also their fluctuational properties (and consequently such characteristics as cross-section self-shielding factors) will reproduce precisely those quantities observed in integral experiments over the wide energy range important for hard-spectrum systems. The total number of resonances for the nuclei concerned here lies within the limits of the permissible.

Another problem occurring when describing the cross-section component governed by s-resonances is the introduction of a single potential scattering radius for the whole of the energy region under consideration. A good description of the total cross-section curves over a wide energy range in the resolved resonance region with a single radius calls for the introduction of

remote resonances (located outside the region under analysis), whose characteristics are normally insufficiently well known. However, they have a significant effect on the mean cross-section level and its energy dependence over a wide energy range. These approaches are tantamount to introducing an energy dependence of the potential scattering radius. Allowance for remote resonances makes it possible to dispense with the introduction of a background component in the scattering and total cross-sections.

Since inter-resonance interference effects for iron isotopes are substantial, the choice of calculational formulae in the resolved resonance region is of great importance. As calculations have shown, the use of the Breit-Wigner multi-level formula for ^{56}Fe is largely unjustified. The principal drawbacks to its use are as follows: under conditions of appreciable inter-resonance interference it strongly distorts the shape of resonances, does not reproduce the cross-section minima and leads to a considerable redistribution of cross-sections even with a broad-group representation. Furthermore, the analysis of the most recent experiments in the resolved resonance field was carried out in the context of the Reich-Moore formalism, taking account of inter-resonance interference in the best approximation. Accordingly, the use of this formalism in a consequential evaluation is inevitable.

Below we shall consider the peculiarities of the evaluations for individual iron isotopes.

^{56}Fe . Using "pseudo-isotopes", the resolved resonance region for the s-wave of ^{56}Fe is 10^{-5} eV-850 keV, i.e. it extends as far as the threshold of inelastic scattering, while for the p- and d-waves it has an upper limit of 350 keV. In the 350-850 keV range the contribution of p- and d-waves is presented in terms of the average resonance parameters, depending on energy and established at points 50 keV apart. The potential scattering radius is taken as 5.0 fm, i.e. equal to the radius of the channel as derived upon analysis of the total cross-sections over a wide energy region [6]. The

sequence of negative and positive s-resonances located outside the 10^{-5} eV-850 keV region was generated on the basis of mean resonance parameters; then the positions and widths of a number of remote resonances were so varied as to describe the cross-section at the thermal point and the level of the mean cross-section in groups located at the boundaries of the resolved resonance region. The parameters of the first p- (1.15 keV) and s-resonances (27.74 keV), having a strong bearing on the iron capture cross-section in fast reactors, were selected in accordance with the recommendations of the international group [7] engaged in analysis and evaluation of the p-wave resonance parameters, and also with the results of the latest experiments [8] for the s-resonance (Table 1). As shown in Fig. 2, by applying the parameter data within the framework of the Reich-Moore approximation a satisfactory description is obtained of the experimental data on the interference minimum in the total cross-section for the 27.74 keV resonance, while calculations under the multi-level Breit-Wigner formula significantly exaggerate the cross-section at the minima. The position and neutron widths of the resolved resonances for energies above 350 keV are taken from Ref. [6], and for energies below this level from Ref. [9].

Figure 3,a shows the curves for the build-up of the sums of resonance numbers for s-, p- and d-waves for ^{56}Fe . There would appear to be some omission of weak d-resonances, but their contribution to the total cross-section and the elastic scattering cross-section is negligible.

Figure 2,b presents the results of calculating the contribution to the total cross-section by the s-wave at zero temperature, reckoned from the resonance parameters [6] in the context of the Reich-Moore formalism and the multi-level Breit-Wigner formula. Since the parameters themselves are derived in the Reich-Moore approximation, the "flow" representation obtained in the context of this formalism describes the shape of the total s-wave cross-section observed experimentally, and the difference in the description yielded by the multi-level Breit-Wigner formula characterizes the degree of

error in the description of the cross-sections occurring upon its use under conditions of appreciable inter-resonance interference. The divergences in the cross-section minima are strongest when calculating the self-shielding factors.

The radiation widths attributed to the resolved resonances are normally based on known values of the areas under the resonances in the capture cross-sections [9] and on the mean radiation width values for the s-, p- and d-resonances determined by analysis for those resonances where they are known.

The mean resonance parameters for the lower boundary of the p- and d-wave unresolved resonance region ($E = 350$ keV) were initially determined by averaging the resolved resonance parameters (Table 2, values in brackets). The capture cross-section calculated using these parameters is in good agreement with the value derived experimentally. However, a part of the parameters thus determined [e.g. the mean distance between resonances with spin $I^\pi = (5/2)^+$] does not agree with existing views on their possible dependence on spin and parity. Subsequently therefore, using the EVPAR [10] program, a correction was effected and a set of average resonance parameters for p- and d-waves was determined which on the one hand was based on parameters derived by averaging in the resolved resonance region and on the other hand did not contradict current conceptions regarding their dependence on spin and parity. The parameters found are given in Table 2 for the extreme energies in the unresolved resonance region. The significant difference in the density of states with the same spin but different parity is worthy of note.

The ENDF-V library format does not permit explicit consideration of the f-wave, whose contribution to the capture cross-section at the upper boundary of the unresolved resonance region becomes appreciable. Allowance for the f-wave contribution is effected by raising the mean radiation widths of the d-wave with change in energy, which is probably preferable to adding a smooth component to the cross-section. Data for the s-wave are not given in Table 2,

since its contribution to this region (350–850 keV) is derived from resolved resonances.

In Table 3 the cross-sections at the thermal point restored from the resonance parameters are compared with the results of evaluation [11].

⁵⁴Fe. The resolved resonance region for the s-wave of this isotope is 10^{-5} eV–500 keV, and for the p- and d-waves this region lies within the range 10^{-5} eV–200 keV, while from 200 to 500 keV the contribution of these waves to the cross-section is represented in terms of the mean resonance parameters. The potential scattering radius is taken as 5.0 fm for the whole resonance region. The cross-sections in the resolved and unresolved resonance region are restored on the basis of the given parameters without using any background components.

The positions of the resolved resonances were taken from Ref. [11], and the set of s-resonance neutron widths was based on the results of study [12]. In the case of the p- and d-resonances an analysis was made of the entire data on widths and the values derived therefrom. Here, the neutron and radiation widths, where they were unknown, were so selected as to describe the quantities A_{γ}^r , measured in Ref. [13], whereas the radiation widths of the individual resonances probably did not appreciably differ from the average radiation width value for the resonances of the given wave. Since considerable omission of d-resonances occurred, leading to an underestimation of the capture cross-section in comparison with that observed in experiments with "poor" resolution (particularly in the 100–200 keV region), the d-level system was supplemented by 24 resonances with the mean width values attributed to them. Unlike the resonances observed experimentally, these are identified in the file by the figure 9 as last significant digit in the resonance energy. The accumulating sums of the resonance numbers for the s-, p- and d-waves allowing for correction for the d-wave resonance system in ⁵⁴Fe are shown in Fig. 3,b. For a correct description of the total cross-section near the upper limit of the resolved resonance region for the s-wave, remote

positive resonances are introduced. In connection with the "flow" representation of the cross-sections in the resolved s-resonance region, the use of the Reich-Moore formalism is recommended, as in the case of the ^{56}Fe isotope.

The cross-sections in the unresolved resonance region for p- and d-waves are described using the mean resonance parameters obtained in the EVPAR-program processing of the average values from the resolved resonance region, which are given in brackets in Table 2. Both sets of parameters yield a good description of the capture cross-section observed in this region. Table 3 presents the values for the cross-sections at the thermal point, yielded by calculation from the resonance parameters.

^{57}Fe is the only stable isotope of iron having a low (14.7 keV) inelastic scattering threshold. The resolved resonance region for waves with different orbital moments was regarded as the single range from 10^{-5} eV to 200 keV, and the unresolved resonance region as the range from 200 to 500 keV. The potential scattering radius was taken as 5.9 fm for the resolved and 5.0 fm for the unresolved resonance region.

The positions and radiation widths of the resolved resonances are defined in Ref. [14], and the neutron widths of the s-resonances for the elastic and inelastic channels in Ref. [15]. The neutron width of the elastic scattering channel for p- and d-resonances was selected from the totality of the experimental data on one or other resonance, including the areas under the capture curve, the assumed mean radiation and reduced neutron widths and also possible spin and parity distributions. The resulting identification of resonances is of course extremely hypothetical, although it does not contradict the existing body of experimental data. Figure 3,c shows the cumulative sums of resonance numbers derived for ^{57}Fe in the resolved resonance region. In accordance with the requirements of the ENDF-V format, file 3 for the total cross-section in the resolved and unresolved resonance region will contain a component having resonance form in the resolved

resonance region and giving the inelastic scattering cross-section in this region.

The mean resonance parameters for the unresolved resonance region were obtained by averaging over the resolved resonance area and are given in Table 2. The competing widths describing inelastic scattering in the unresolved resonance region take effective account of the contribution from a number of inelastic scattering levels for those spin states and energies where this is appreciable.

Table 3 shows the cross-section values at the thermal point derived from the resonance parameters.

⁵⁸Fe is the least thoroughly studied of the stable isotopes of iron. Since its content in a natural mixture is only 0.28%, even substantial imprecision in its cross-sections does not have an appreciable effect on the cross-sections for natural iron.

As basis for the evaluation in the resolved resonance region (from 10^{-5} eV to 200 keV) use was made of the parameter values given in Ref. [11]. Only the contribution from the s- and p-waves were considered in the resolved resonance region. The p-resonance radiation widths for which they are unknown were regarded as equal to the mean values obtained by averaging known widths for p-resonances, and then were so varied as to describe the mean capture cross-section level, known from experiments with low resolution. Figure 3,d shows the cumulative sum of resonance numbers for s- and p-waves in the resolved resonance region for ⁵⁸Fe.

The unresolved resonance region was regarded as that between 200 and 500 keV. The mean neutron widths and the distances between the levels were originally derived from averaging the parameters in the resolved resonance region, and the mean radiation widths were preliminarily evaluated from the systematics of these widths (see Table 2). Use was then made of the EVPAR program to make slight corrections to the s- and p-resonance parameters, while the d-wave parameters were selected with reference to the description of

the cross-sections derived in experiments with poor resolution. The cross-sections at the thermal point obtained from the resonance parameters are given in Table 3.

Natural iron. The cross-sections for a natural mixture of iron isotopes were obtained by summing all the stable isotopes entering into the composition of iron with the following contents: ^{56}Fe - 91.72%; ^{54}Fe - 5.8%; ^{57}Fe - 2.2%; ^{58}Fe - 0.28%. Hence the evaluation of natural iron in the resolved and unresolved resonance region was co-ordinated with the evaluations for the individual iron isotopes. The following features of the proposed evaluation are worthy of note:

1. The capture cross-section in the group 4.65-10 keV is approximately 30% lower than the values given in other evaluations (see Fig. 1), and is confirmed by the results of measurements on a lead cube. It is necessary to increase the capture cross-section in this group for ^{54}Fe , which accounts for the principal contribution to this region (approximately by 60%), in order to obtain such a high level for the cross-section in respect of natural iron. However, the parameters of the two ^{54}Fe resonances making a contribution to this group are fairly well known and cannot be appreciably changed;
2. The total cross-section for energies 1-40 keV is higher, and for the region 40-200 keV is lower, than all other evaluations. This would seem to be associated with the fact that, over the broad energy range 10^{-5} eV-850 keV, the calculations for ^{56}Fe were effected with a single scattering potential radius, 5 fm. However, the mean cross-section level itself in this region needs experimental refinement.

REFERENCES

1. ENDF/B Summary Documentation, BNL-17541, 1973.
2. Bychkov V.M., Vozyakov V.V., Manokhin V.N. et al. Yad. Konst., 1974, issue 19, part 1, p. 46 (in Russian).
3. Howerton R.J., Dye R.E., Perkins S.T. Rep. UCRL-50400, v. 4, rev.1, appendix C, 1982.
4. Summary of JEMDL-2 general purpose file. Ed. by T.Nakagawa; JAERI-M-84-103, 1984, p.150.
5. Cullen D.E. In: Nucl. data for structural materials: Proc. of the IAEA consultants meeting: INDC(NDS)-152/L, 1984, p.150.
6. Cornelis E.M., Mewissen L., Poortmans F. In: Nucl. data for Sci. and technol.: Proc. of the intern. conf. (Antwerp., 1982). Holland, 1983, p.135.
7. Perey F.G.J. In: [5], p.46.
8. Wisshak K., Käppeler F. Ibid., p.46.
9. Corvi P., Brusegan A., Buyl R., Rohr G. Ibid. p.31.
10. Manturov G.N., FEHI Preprint No. 666. Obninsk 1976 (in Russian).
11. Mughabghab S.P., Divadeenam M., Holden N.E. Neutron Cross-Sections, v.1, part A. Academic Press, 1981.
12. Moxon M.C., Brisland J.B. In: Neutron data of structural materials for fast reactors: Proc. of specialist meeting. Geel, 1977, p.689.
13. Brusegan A., Corvi P., Shelley R. e.e. In: [6], p.135.
14. Rohr G., Brusegan A., Corvi P. e.e. Ibid., p.139.
15. Rohr G., Müller K.K. Z. Phys., 1969, v.227, p.1.

Paper received by editors on 18 December 1985.

Table 1. Parameters of first p- and s-resonances for ^{56}Fe

Parameter	p-resonance	s-resonance
Resonance energy, keV	1.15	27.74
Spin of parity I^π	$(1/2)^-$	$(1/2)^+$
Neutron width Γ_n , eV	0.0617	1474.0
Radiation width Γ_γ , eV	0.574	1.06

Table 2. Mean distances between levels $\langle D \rangle$ (in keV) and mean widths $\langle \Gamma_n^0 \rangle$, $\langle \Gamma_{n'} \rangle$, $\langle \Gamma_\gamma \rangle$ (in eV) for boundary energy values in the unresolved resonance region of iron isotopes

$^{56}\text{Fe}, I^\pi = 0^+$												
E_n , keV	$l = 1$						$l = 2$					
	$I^\pi = (1/2)^-$			$I^\pi = (3/2)^-$			$I^\pi = (3/2)^+$			$I^\pi = (5/2)^+$		
	$\langle D \rangle$	$\langle \Gamma_n^0 \rangle$	$\langle \Gamma_\gamma \rangle$	$\langle D \rangle$	$\langle \Gamma_n^0 \rangle$	$\langle \Gamma_\gamma \rangle$	$\langle D \rangle$	$\langle \Gamma_n^0 \rangle$	$\langle \Gamma_\gamma \rangle$	$\langle D \rangle$	$\langle \Gamma_n^0 \rangle$	$\langle \Gamma_\gamma \rangle$
350	13,2	0,248	0,64	6,60	0,124	0,53	10,6	1,77	0,49	7,06	1,18	0,37
	(14,3)	(0,266)	(0,58)	(8,50)	(0,164)	(0,58)	(10,0)	(1,68)	(0,8)	(27,0)	(4,02)	(0,8)
850	9,22	0,17	0,77	4,58	0,084	0,64	7,40	1,18	1,54	4,88	0,78	1,16

$^{54}\text{Fe}, I^\pi = 0^+$												
E_n , keV	$l = 1$						$l = 2$					
	$I^\pi = (1/2)^-$			$I^\pi = (3/2)^-$			$I^\pi = (3/2)^+$			$I^\pi = (3/2)^+$		
	$\langle D \rangle$	$\langle \Gamma_n^0 \rangle$	$\langle \Gamma_\gamma \rangle$	$\langle D \rangle$	$\langle \Gamma_n^0 \rangle$	$\langle \Gamma_\gamma \rangle$	$\langle D \rangle$	$\langle \Gamma_n^0 \rangle$	$\langle \Gamma_\gamma \rangle$	$\langle D \rangle$	$\langle \Gamma_n^0 \rangle$	$\langle \Gamma_\gamma \rangle$
200	10,3	0,44	0,75	5,14	0,22	0,64	10,4	1,73	0,64	6,90	1,15	0,50
	(9,87)	(0,40)	(0,64)	(6,58)	(0,50)	(0,64)	(8,20)	(1,37)	(1,0)	(23,6)	(9,50)	(1,0)
500	8,41	0,35	0,83	4,19	0,17	0,71	8,46	1,39	0,71	5,61	0,92	0,55

$^{57}\text{Fe}, I^\pi = (1/2)^-$																
E_n , keV	$l = 0$							$l = 1$								
	$I^\pi = 0^-$				$I^\pi = 1^-$			$I^\pi = 0^+$				$I^\pi = 1^+$				
	$\langle D \rangle$	$\langle \Gamma_n^0 \rangle$	$\langle \Gamma_{n'} \rangle$	$\langle \Gamma_\gamma \rangle$	$\langle D \rangle$	$\langle \Gamma_n^0 \rangle$	$\langle \Gamma_{n'} \rangle$	$\langle \Gamma_\gamma \rangle$	$\langle D \rangle$	$\langle \Gamma_n^0 \rangle$	$\langle \Gamma_{n'} \rangle$	$\langle \Gamma_\gamma \rangle$	$\langle D \rangle$	$\langle \Gamma_n^0 \rangle$	$\langle \Gamma_{n'} \rangle$	$\langle \Gamma_\gamma \rangle$
200	26,3	8,31	0,0	1,9	12,4	5,95	1897	2,1	26,3	0,7	29	0,69	8,77	0,31	31,8	0,65
500	26,3	8,31	0,0	1,9	12,4	5,95	4651	2,1	26,3	0,7	131	0,69	8,77	0,31	167	0,65

E_n , keV	$l = 1$							$l = 2$								
	$I^\pi = 2^+$				$I^\pi = 1^-$			$I^\pi = 2^-$				$I^\pi = 3^-$				
	$\langle D \rangle$	$\langle \Gamma_n^0 \rangle$	$\langle \Gamma_{n'} \rangle$	$\langle \Gamma_\gamma \rangle$	$\langle D \rangle$	$\langle \Gamma_n^0 \rangle$	$\langle \Gamma_{n'} \rangle$	$\langle \Gamma_\gamma \rangle$	$\langle D \rangle$	$\langle \Gamma_n^0 \rangle$	$\langle \Gamma_{n'} \rangle$	$\langle \Gamma_\gamma \rangle$	$\langle D \rangle$	$\langle \Gamma_n^0 \rangle$	$\langle \Gamma_{n'} \rangle$	$\langle \Gamma_\gamma \rangle$
200	5,26	0,27	34,5	0,61	16,6	1,85	1890	1,5	10	0,64	2990	1,26	7,14	0,4	1000	1,26
500	5,26	0,27	202	0,61	16,6	1,85	4651	1,5	10	0,64	7330	1,26	7,14	0,4	2640	1,26

$^{58}\text{Fe}, I^\pi = 0^+$															
E_n , keV	$l = 0$			$l = 1$						$l = 2$					
	$I^\pi = (1/2)^+$			$I^\pi = (1/2)^-$			$I^\pi = (3/2)^-$			$I^\pi = (3/2)^+$			$I^\pi = (5/2)^+$		
	$\langle D \rangle$	$\langle \Gamma_n^0 \rangle$	$\langle \Gamma_\gamma \rangle$	$\langle D \rangle$	$\langle \Gamma_n^0 \rangle$	$\langle \Gamma_\gamma \rangle$	$\langle D \rangle$	$\langle \Gamma_n^0 \rangle$	$\langle \Gamma_\gamma \rangle$	$\langle D \rangle$	$\langle \Gamma_n^0 \rangle$	$\langle \Gamma_\gamma \rangle$	$\langle D \rangle$	$\langle \Gamma_n^0 \rangle$	$\langle \Gamma_\gamma \rangle$
200	21,5	6,90	1,20	18,0	1,06	0,44	8,98	0,53	0,38	10,7	1,06	0,30	7,12	0,70	0,23
	(21)	(6,9)	(1,2)	(18)	(1,1)	(0,4)	(9,0)	(0,5)	(0,4)	-	-	-	-	-	-
500	17,3	3,05	1,34	14,5	0,82	0,50	7,23	0,41	0,42	8,62	0,64	0,61	5,72	0,56	0,47

Table 3. Thermal cross-sections ($E_n = 0.253$ eV) on iron isotopes

Isotope	TsYaD-2		MDH-81	[11]
	σ_B	σ_f	σ_B	σ_f
^{54}Fe	2,16	2,14	$2,17^{*}_{-0,10}$	$2,25^{*}_{-0,18}$
^{56}Fe	12,27	2,63	$12,46^{*}_{-0,49}$	$2,59^{*}_{-0,14}$
^{57}Fe	2,13	2,44	-	$2,49^{*}_{-0,30}$
^{58}Fe	3,19	1,27	-	$1,28_{-0,05}$

[*] Cross-sections averaged over the thermal spectrum.

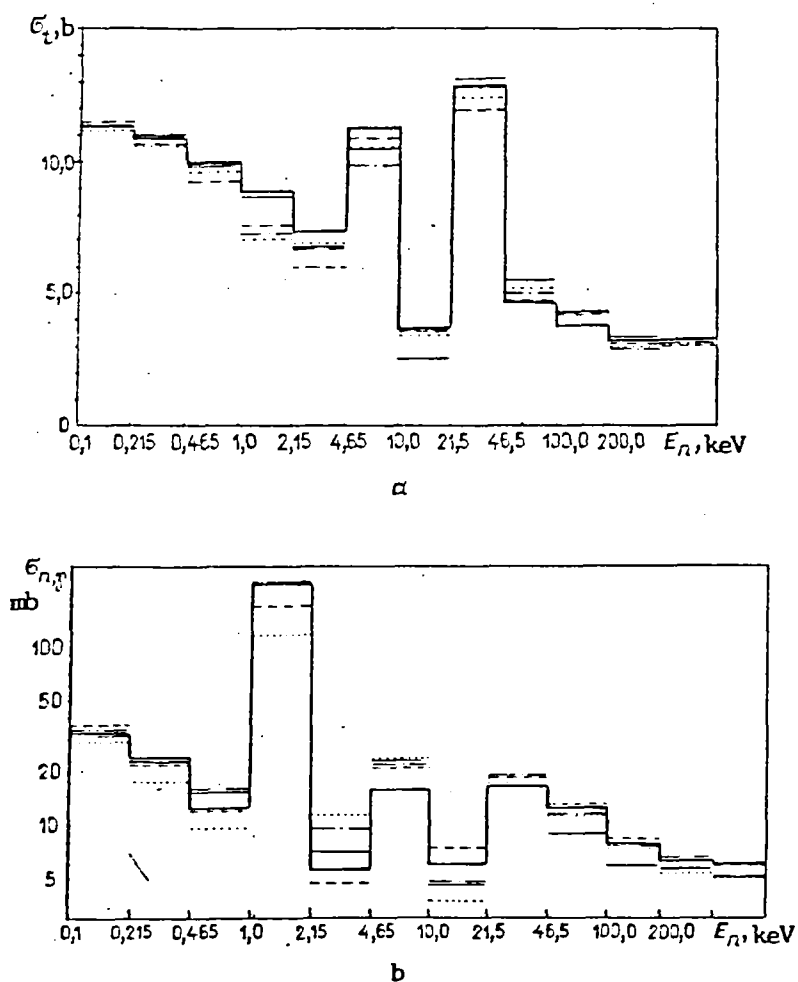


Fig. 1. Comparison of total cross-sections (a) and capture cross-sections (b) for natural iron on the basis of various libraries of evaluated neutron cross-sections in a 26-group representation: — - TsYaD-2; ···· - TsYaD-1; - - - - BNAB-78; — · — ENDFB-IV; - - - - JENDL-II.

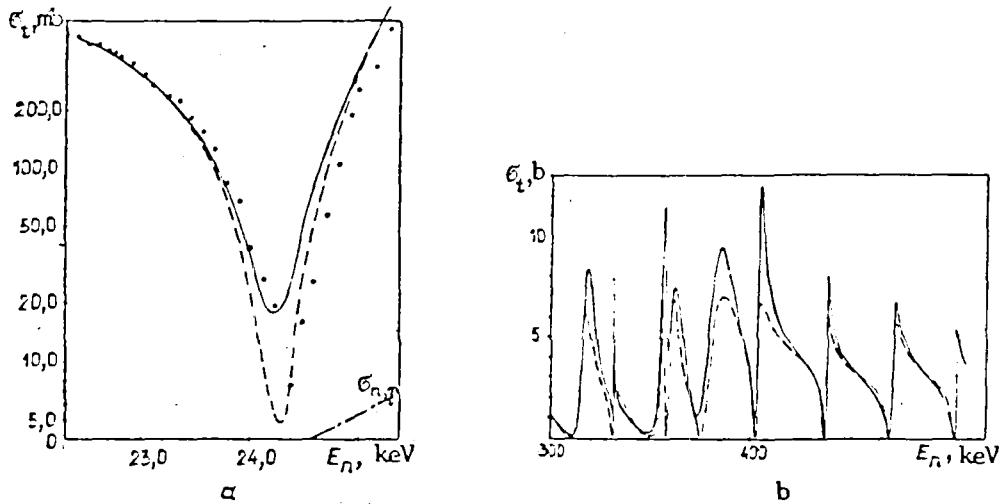


Fig. 2.

Description of the total cross-section for ^{56}Fe in the interference minimum region of the s-resonance (a) and the broader energy region (b) at 27.74 keV in the context of the Breit-Wigner multi-level formula (continuous curve) and the Reich-Moore formalism (dotted curve). The points represent experimental data.

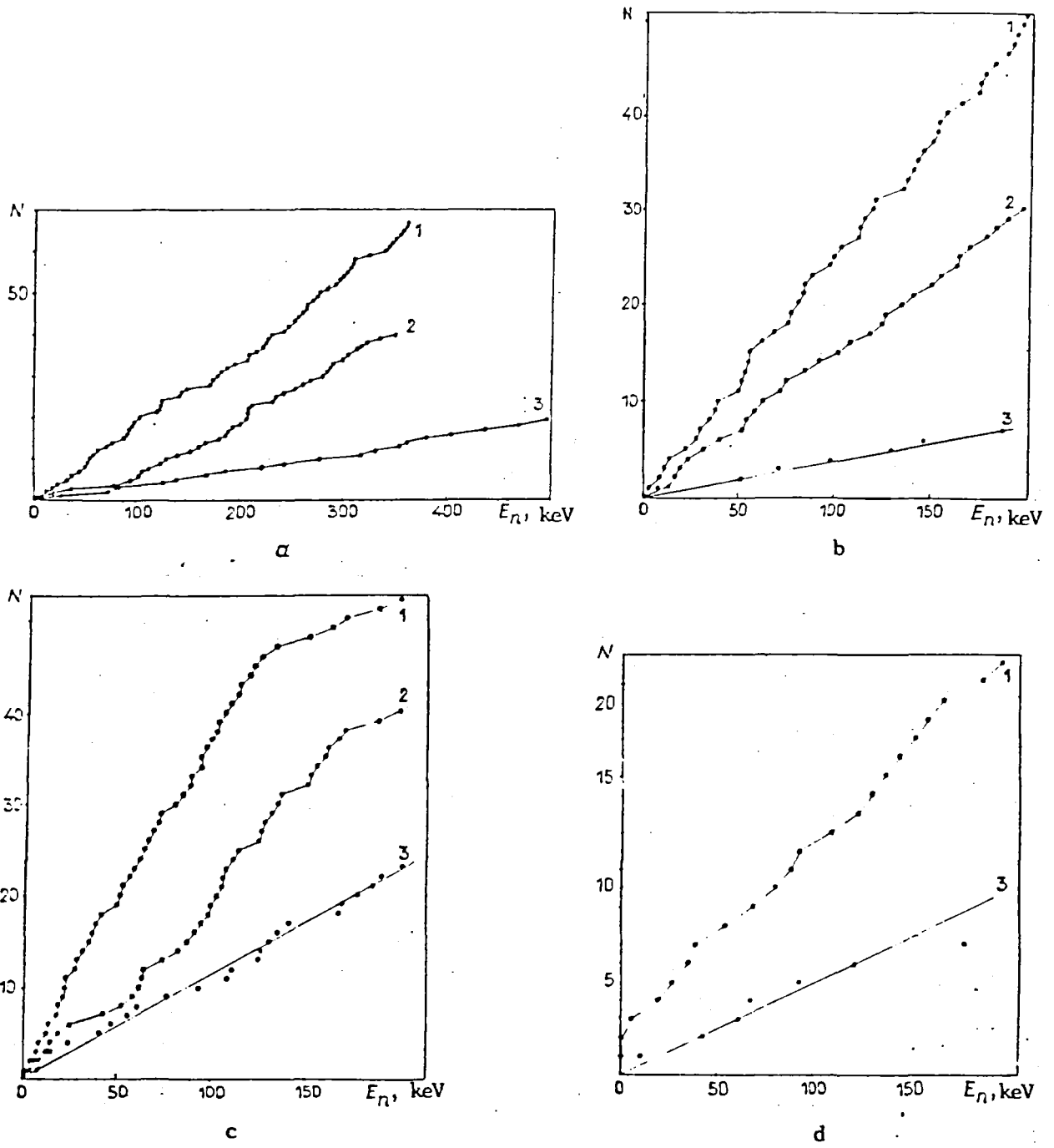


Fig. 3. Cumulative sums of resonance numbers for p-waves (curve 1, $l = 1$), the d-wave (curve 2, $l = 2$) and the s-wave (curve 3, $l = 0$) in respect of isotopes ^{56}Fe (a), ^{54}Fe (b), ^{57}Fe (c) and ^{58}Fe (d). For purposes of clarity the points corresponding to the number of resonances for a given energy are joined by lines or a straight line is drawn through them.

SCATTERING OF 6 MeV NEUTRONS ON VANADIUM

A.V. Polyakov, G.N. Lovchikova, V.A. Vinogradov,
B.V. Zhuravlev, O.A. Sal'nikov, S.Eh. Sukhikh

Vanadium is foreseen as a structural material in the blankets of thermonuclear reactors, forming part of the envelope separating the thermonuclear plasma zone and the heat release and tritium breeding zone. According to the list of required data [1], there is a need, in the case of vanadium, for scattered neutron energy and angular distributions in the energy region of several megaelectron volts. The required precision in respect of elastic scattering angular distributions is 10%, and in respect of secondary neutron energy spectra 15%. The present work was performed on the basis of these requirements.

The spectra of neutrons scattered on natural vanadium were measured with a neutron spectrometer working by time-of-flight [2] in association with an EhGP-10M accelerator. As neutron source use was made of the ${}^3\text{T}(p,n){}^3\text{He}$ reaction, with a gaseous tritium target. The initial energy of the neutrons incident on the sample was 6.07 ± 0.07 MeV. The features of the gaseous target are described in detail in Ref. [3]. The neutron detector consisted of a stilbene crystal (diameter 6.3 cm and thickness 3.9 cm), viewed by an FEhU-30 photomultiplier. In order to reduce the background the detector was located in a shielding whose design is described in Ref. [2]. The distance between detector and sample was 1.98 m. The sample, natural vanadium, was placed at a distance of 16.5 cm from the target centre, and took the form of a hollow cylinder of mass 120 g, height 5 cm, external diameter 3 cm and internal diameter 2 cm.

The yield of neutrons from the target was monitored by a neutron detector, similar to the basic detector; it was placed at an angle of 45° to the direction of the accelerated protons at a distance of 3 m from the target centre. Normalization of the scattered neutron spectra and monitoring of

spectrometer operation were effected by reference to the monochromatic neutron peak. As additional monitor use was made of an all-wave counter. The stability of operation of detector, monitor and all-wave counter were checked by periodical measurements of the number of radioactive source events recorded over a given period of time. Stability of operation of the detector and monitor was at the 1.5% level, and that of the all-wave counter at the 1% level.

The absolute efficiency of neutron recording by the detector in the energy range from recording threshold up to 7 MeV was determined by comparing the experimental and calculational spectra of prompt neutrons from ^{252}Cf spontaneous fission. The calculational spectrum was described by a Maxwellian distribution with parameter $T = 1.42$ MeV. The root mean square error of the results of the series of measurements amounted to 2-5% in the escaping neutron energy range 0.5-7 MeV. The detector neutron recording threshold was 0.4 MeV.

The block diagram and the operating principle of the spectrometer electronics are set forth in Ref. [4]. The channel width of the time converter was 0.503 ns, and its differential and integral non-linearity were not poorer than 1 and 0.5% respectively. The total time resolution of the spectrometer, determined from the half-height width of the gamma peak, over a flight path of 1.98 m, was 3 ns.

The absolute values of the cross-sections for neutron elastic and inelastic scattering were derived by normalizing for the (n-p)-scattering cross-section on hydrogen [5]. For this purpose measurements were made at an angle of 45° to the direction of motion of the protons in a polyethylene sample (height 5 cm, diameter 1 cm). The polyethylene scatterer was located in the same place as the vanadium sample.

By means of a Monte Carlo method using the programme described in Ref. [6], a correction was calculated for the attenuation and multiple scattering of neutrons in the vanadium sample. The procedure for studying the scattered neutron spectra on the vanadium consisted of a series of

measurements with and without the sample at angles of 30°, 45°, 60°, 90°, 120° and 150° with an evacuated target and with a target filled with tritium to a pressure of about 2.02×10^5 Pa. At the beginning of each series, measurements were made of the direct flux spectrum at an angle of 0°.

Figure 1 shows the time spectrum of neutrons scattered on vanadium, measured at an angle of 120° and a neutron energy of 6.07 MeV. On the spectrum are visible groups of neutrons corresponding to excitation of vanadium levels, and the elastically scattered neutron peak. Separation of the elastic and inelastic neutron scattering processes was effected with reference to the shape of the direct flux spectrum by the method described in Ref. [7].

The differential cross-sections for elastic scattering on vanadium are given in Fig. 2. The results of the present work and of that described in Ref. [8], obtained at the same neutron energy, coincide within the limits of measurement error for angles of 60° and 90°. For angles of 30°, 45°, 120° and 150° the results of the present work are 15-30% higher than those of Ref. [8]. For purposes of comparison the figure shows the results from Ref. [9] obtained for neutron energies of 5.44 and 6.44 MeV.

The spectra at the various angles and the integral spectrum of inelastically scattered neutrons on vanadium at an initial energy $E_0 = 6.07$ MeV are presented in Fig. 3. The group of neutrons corresponding to excitation of levels $Q = -(1.609 + 1.813)$ MeV was separated off. This separation was carried out on the time spectra, it being assumed that the contribution by less energetic and higher energetic neutrons was equal to the contribution from the neutrons of the separated group in the higher energetic and lower energetic neutron regions.

Figure 4 shows the neutron angular distributions derived in the present work, corresponding to excitation of levels $Q = -(1.609 + 1.813)$ MeV, in comparison with the results of Ref. [9]. It will be seen from the figure that at similar initial energies the data from the present work do not contradict those of Ref. [9].

The cross-sections for inelastically scattered neutrons as a function of secondary neutron energy were measured with an accuracy of 6-12%. This error includes the statistical error (2-8%), and also the error - amounting to 6% - due to normalization for the (n-p)-scattering cross-section in polyethylene, the stability of operation of the apparatus, the detector efficiency, the transition from time spectrum to energy spectrum, and subtraction of the elastic peak. The error in separation of the group of neutrons corresponding to excitation of levels $Q = -(1.609 + 1.813)$ MeV was 10-20% for various angles of neutron escape.

The double differential inelastic scattering cross-sections and the angular distributions for neutron elastic and inelastic scattering corresponding to excitation of levels $Q = -(1.609 + 1.813)$ MeV were transmitted to the Nuclear Data Centre of the USSR State Committee on the Utilization of Atomic Energy.

REFERENCES

- [1] WRENDA 83/84: Rep. INDC (SEC)-88 URSF. Vienna: IAEA (1983).
- [2] TRUFANOV, A.M., NESTERENKO, V.S., FETISOV, N.I. et al., Prib. Tekh. Ehksp., No. 2 (1979) 50-55 (in Russian).
- [3] FETISOV, N.I., SIMAKOV, S.P., TRUFANOV, A.M. et al., *ibid.*, No. 6 (1980) 22-25 (in Russian).
- [4] SIMAKOV, S.P., LOVCHIKOVA, G.N., SAL'NIKOV, O.A., At. Ehnerg, Vol. 51, No. 4 (1981) 244 (in Russian).
- [5] SIMAKOV, S.P., LOVCHIKOVA, G.N., SAL'NIKOV, O.A. et al., Vopr. At. Nauk. i Tekh. Ser. Yad. Konst., No. 4(39) (1980) 7 (in Russian).
- [6] POPOV, V.I., KOTEL'NIKOVA, G.V., *ibid.*, No. 16 (1974) 113 (in Russian).
- [7] SIMAKOV, S.P., LOVCHIKOVA, G.N., SAL'NIKOV, O.A. et al., *ibid.*, No. 5(44), (1981) 23 (in Russian).
- [8] HOLMQUIST, B., JOHANSSON, S.G., LODIN, G., WEIDLING, T., Nucl. Phys., v. A146 (1970) 321.
- [9] PEREY, P.G., KINNEY, W.E., Rep. ORNL-4551, Oak Ridge (1970).

Paper received by editors on 31 January 1986.

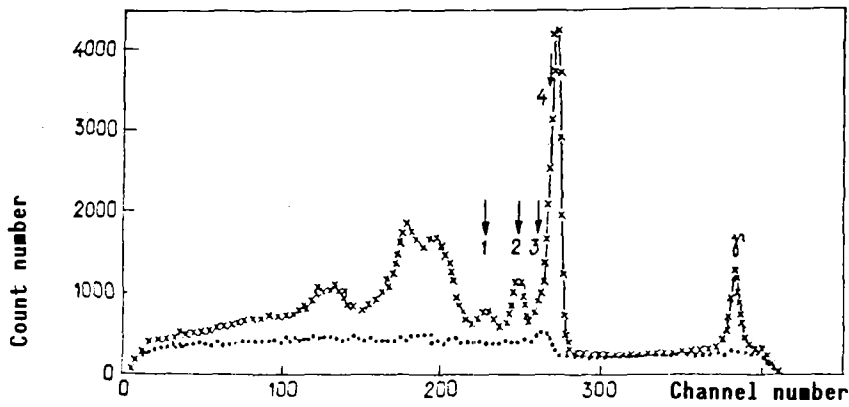


Fig. 1. Time spectra of neutrons with sample (x) and without sample (o) measured at an angle of 120° with a tritium filled target. The value of Q for the group of levels:
 1 - $Q = -(2.409 + 2.545 + 2.675 + 2.699 + 2.790)$ MeV;
 2 - $Q = -(1.609 + 1.813)$ MeV; 3 - $Q = -0.930$ MeV;
 4 - $Q = -0.320$ MeV.

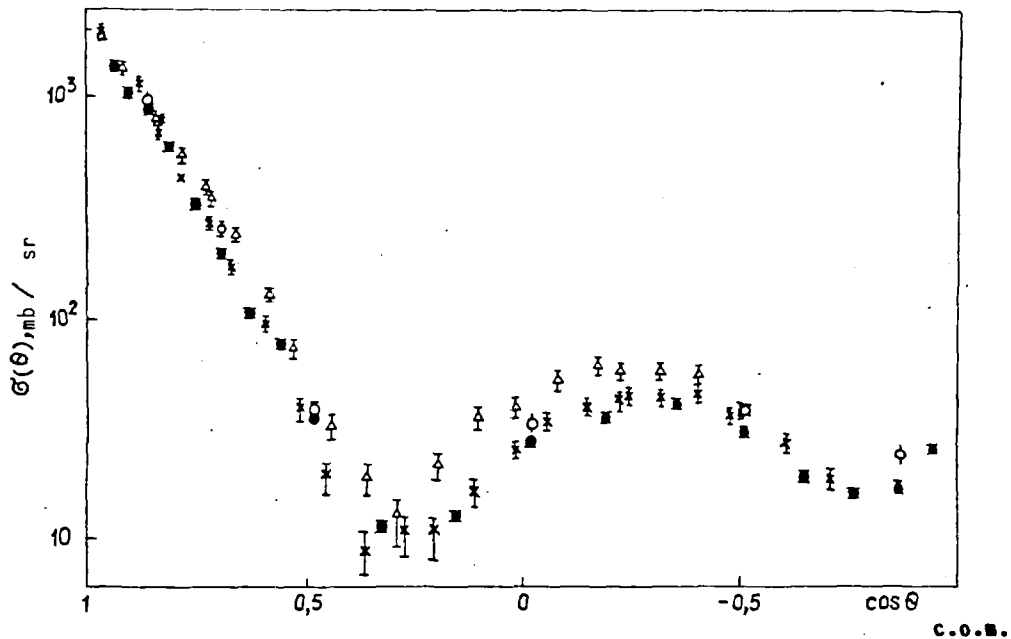


Fig. 2. Angular distributions of neutrons inelastically scattered on vanadium. Data from studies: o - the present work ($E_0 = 6.07$ MeV); • - [8] ($E_0 = 6.09$ MeV); Δ - [9] ($E_0 = 5.44$ MeV); x - [9] ($E_0 = 6.44$ MeV).

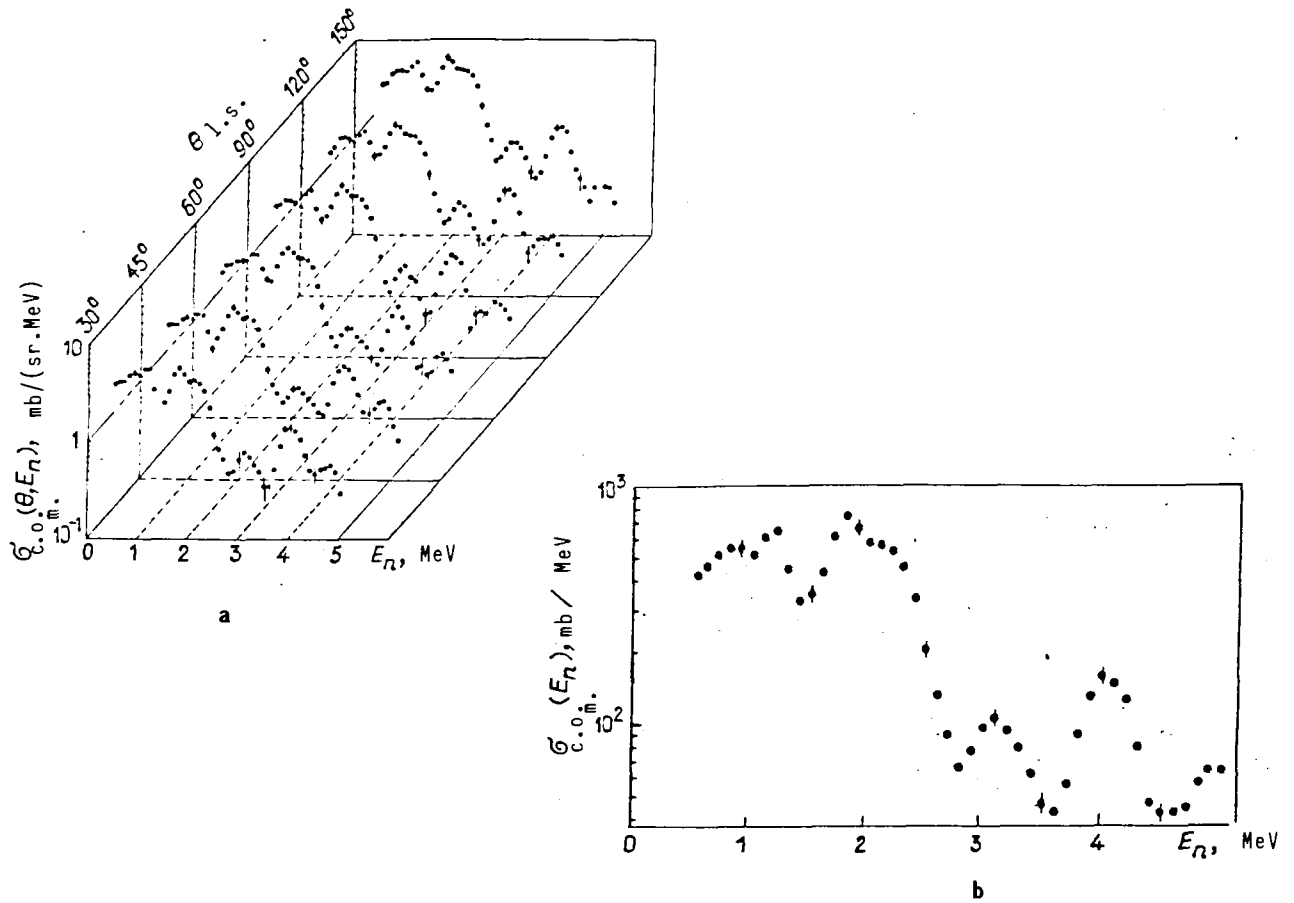


Fig. 3. Double differential cross-sections (a) and integral spectrum (b) for neutrons inelastically scattered on vanadium.

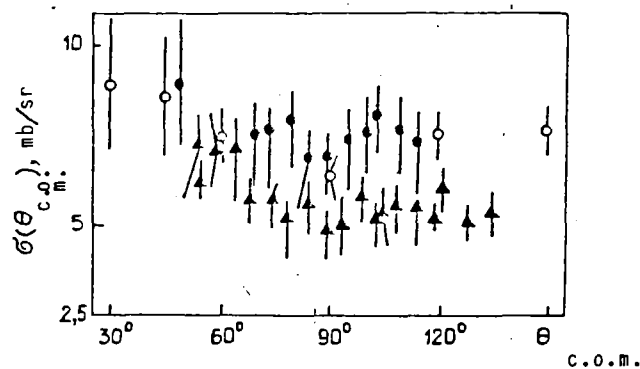


Fig. 4. Angular distributions of inelastically scattered neutrons. Data from references: o - the present work ($E_0 = 6.07$ MeV); ● - [9] ($E_0 = 5.44$ MeV); ▲ - [9] ($E_0 = 6.44$ MeV).

INELASTIC SCATTERING OF NEUTRONS ON ^{93}Nb NUCLEI

Yu.A. Nemilov, Ya.M. Kramarovskij, E.D. Teteren, L.P. Pobedonostsev

Niobium is a promising material for use in various nuclear reactor components. This element possesses such valuable properties as a high melting point, a relatively low neutron capture cross-section, and ease of machining. The inelastic scattering of neutrons on ^{93}Nb nuclei has been studied in Refs [1-3], but in these works there are appreciable discrepancies between the values obtained for the cross-sections. Thus, in Ref. [1] the cross-section for the $^{93}\text{Nb}(n,n'\gamma)$ reaction with excitation of a level at 809.8 keV in the neutron energy range 1-2 MeV is as much as 125 mb, whereas in Ref. [3], in the same energy range, the cross-section obtained does not exceed 75 mb. There are also divergences in the ^{93}Nb nuclear level systems employed, and in the γ -transitions between them: in Ref. [1] no level appears or is referred to with an excitation energy of 686.8 keV, but it does appear in Ref. [3]. We therefore performed measurements of neutron inelastic scattering cross-sections at energies of 780-2200 keV with excitation of a number of low levels of the ^{93}Nb nucleus. The measurement procedure was similar to that described in Ref. [4]. The neutron source was the T(p,n) reaction, and the target thickness was about 1 mg/cm^2 . The sample, of high purity metallic niobium in the form of a cylinder 18 mm in diameter and 27 mm in height, was placed at a distance of 10 cm from the target. The γ -photons were recorded by a Ge(Li) detector with volume 45 cm^3 , located within a shielding of lead and hydrogenous materials. The detector resolution was 4.5 keV for ^{60}Co lines.

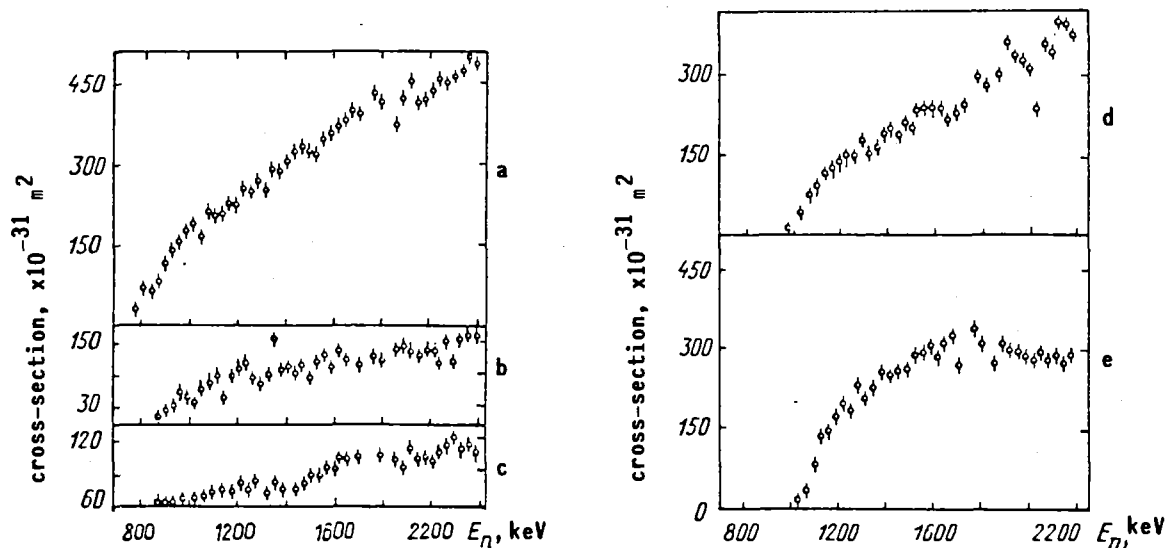
Detector efficiency was calibrated with reference to ^{137}Cs and ^{152}Eu sources, which were put in place of the sample being investigated. The neutron flux to the target during the measurement time was determined from counting fission fragments in a miniature ionizing chamber with a known quantity of ^{235}U , attached to the sample being studied. In determining the number γ -photons recorded, we made corrections for the finite dimensions of

the sample in accordance with the data contained in Ref. [5]. When determining the cross-sections for the $^{93}\text{Nb}(n,n'\gamma)$ reaction with excitation of number of low energy levels of this nucleus we made direct use of the γ -lines observed in the experiment. Here, great attention was devoted to finding those γ -lines which may be associated with the populating of the states under investigation as a result of transitions from more highly excited states (see Table and Figure). The ^{93}Nb excitation functions measured in the present work for the states at 743.7, 808.4, 809.8, 949.6 and 978.6 keV did not substantially differ in shape from similar curves shown in Ref. [3]. However, in the case of the 743.7 and 949.6 keV states a smaller cross-section is observed in Ref. [3] when $E > 1.6$ MeV, while for the 808.4 keV state and with $E < 1.4$ MeV a cross-section emerges in Ref. [3] which is larger than in the present work.

REFERENCES

1. Rogers V.C., Beghian L.E., Glikeman P.M. Nucl. Phys., 1970, v.A142, N 1, p.100-112.
2. Gobel H., Feicht E.J. Z. Phys., 1970, v.240, N 5, p.430.
3. Heerden J. van, McMurray W.R. Ibid., 1973, v.260, N 1, p.9-34.
4. Nesilov Yu.A., Pobedonostsev L.A., Yeterin E.D. At. Ehnerg., 1982, Vol. 53, No. 3 (in Russian).
5. Dickens J.K. Nucl. Instrum. and Methods, 1972, v.98, N 3, p.451-454.

Paper received by editors on 16 August 1985.



Inelastic scattering cross-section for neutrons on ^{93}Nb nuclei with excitation of levels, keV: a - 743.7; b - 808.4; c - 809.8; d - 949.6; e - 978.6

Cross-sections (and their errors) for excitation of six levels in the
 reaction $^{93}\text{Nb}(n,n')$, $\times 10^{-31} \text{ m}^2$ (mb)

Neutron energy keV	Level-excitation energy					
	686.8 keV; (1/2-, 3/2-)	743.7 keV; 7/2+	808.4 keV; 5/2+	809.8 keV; 5/2-	949.6 keV; 13/2+	978.6 keV; 11/2+
780	-	32(5)	-	-	-	-
810	-	70(5)	-	-	-	-
840	-	66(7)	-	-	-	-
870	19(5)	83(6)	6(5)	10(5)	-	-
900	23(4)	112(8)	7(4)	26(6)	-	-
930	18(4)	142(13)	10(5)	34(6)	-	-
960	30(5)	186(13)	12(5)	57(5)	-	-
990	22(4)	179(14)	10(5)	47(12)	-	-
1020	29(5)	192(15)	14(5)	40(12)	-	-
1050	29(6)	167(14)	15(4)	64(12)	50(8)	20(8)
1080	24(4)	216(15)	22(7)	74(14)	85(8)	35(8)
1110	-	209(15)	26(7)	91(6)	96(7)	84(8)
1140	28(4)	210(15)	31(10)	49(16)	119(7)	138(7)
1170	19(4)	224(16)	28(7)	91(14)	128(8)	149(9)
1200	-	226(17)	40(5)	98(12)	145(8)	174(9)
1230	33(6)	256(17)	32(6)	110(7)	150(8)	198(9)
1260	24(4)	255(18)	38(14)	84(15)	150(9)	190(10)
1290	30(6)	270(18)	10(7)	82(14)	179(10)	233(10)
1320	31(7)	256(17)	22(7)	90(14)	158(9)	211(9)
1350	32(6)	287(20)	41(6)	158(9)	171(7)	228(8)
1380	29(6)	289(20)	34(6)	98(6)	192(9)	255(9)
1410	-	307(20)	-	101(16)	201(9)	261(9)
1440	-	323(20)	31(10)	95(16)	194(11)	257(12)
1470	25(5)	331(20)	37(13)	108(16)	209(10)	263(11)
1500	36(4)	328(20)	52(13)	85(14)	207(10)	266(11)
1530	-	324(20)	51(10)	116(11)	237(12)	292(14)
1560	32(5)	351(20)	70(12)	123(14)	236(8)	297(8)
1590	29(6)	361(21)	65(15)	107(17)	239(13)	306(14)
1620	48(6)	374(20)	84(9)	138(7)	241(11)	287(12)
1650	41(7)	383(18)	87(9)	120(9)	225(8)	315(10)
1680	-	400(20)	120(12)	125(10)	238(14)	325(18)
1710	-	399(24)	91(14)	109(10)	247(12)	290(14)
1770	83(13)	432(26)	120(17)	124(15)	302(17)	339(18)
1800	108(20)	417(25)	93(16)	125(15)	284(17)	312(18)
1830	-	443(28)	88(15)	133(16)	295(17)	296(18)
1860	-	376(25)	83(12)	141(15)	306(17)	280(15)
1890	-	426(31)	73(13)	142(20)	363(19)	312(18)
1920	-	454(33)	102(12)	137(14)	343(19)	300(17)
1950	-	417(30)	86(9)	133(13)	335(18)	298(20)
1980	-	414(30)	87(10)	138(13)	317(19)	289(21)
2010	-	434(25)	80(12)	140(12)	234(12)	286(22)
2040	-	456(27)	96(10)	111(13)	360(25)	298(22)
2070	-	452(27)	110(12)	152(15)	353(24)	286(22)
2100	-	462(27)	123(12)	110(20)	404(25)	285(23)
2130	-	470(28)	106(8)	150(11)	400(23)	280(22)
2160	-	498(30)	105(8)	153(4)	377(24)	292(21)
2190	-	487(30)	95(6)	160(10)	380(24)	333(18)

INTEGRAL PROMPT FISSION NEUTRON SPECTRUM FROM 1.5 MeV
NEUTRON INDUCED FISSION OF ^{232}Th

S.Eh. Sukhikh, G.N. Lovchikova, V.A. Vinogradov,
B.V. Zhuravlev, A.V. Polyakov, O.A. Sal'nikov

Measurements were made of the prompt fission neutron spectrum under conditions of induced fission of ^{232}Th nuclei by 1.45 MeV neutrons. There has recently been a considerably heightened interest in prompt fission neutron spectra. On the one hand there have emerged new calculational approaches based on application of the progress made in nuclear theory to analysis of prompt fission neutron spectra, and on the other hand there has been an increase in the number of experimental investigations of these spectra [1, 2]. However, studies on measurements of prompt fission neutron spectra occurring upon ^{232}Th fission by fast neutrons are practically non-existent, due to difficulties in carrying out the experiments. Nevertheless, the data in question are necessary for calculating nuclear power facilities, and requests for them are contained in the list of necessary nuclear data [3]. The required accuracy for the data is 10%.

In the present study, measurements were made of the emission spectra for neutrons from ^{232}Th nuclei in the secondary neutron energy range from the detector threshold (0.6 MeV) up to $E_n = 10$ MeV. The emission spectrum in the energy range above the initial bombarding neutron energy level contains only neutrons formed as a result of fission. The emission neutron spectra were measured by the time-of-flight method using a spectrometer associated with an EhGP-10M accelerator, working in the pulsed regime. The neutron source was the $^3\text{T}(p,n)^3\text{He}$ reaction, using a gaseous tritium target. The initial neutron energy incident on the sample was 1.49 ± 0.05 MeV. The design and features of the target are described in detail in Ref. [4]. The mean proton flux to the target was 1 μA at a pulse repetition frequency of 5 MHz. The sample, made of metallic thorium, had the form of a hollow cylinder with external diameter 4.5 cm, internal diameter 4.0 cm and height

5.0 cm, and was located at an angle of 0° to the direction of the proton beam at a distance of 16.8 cm from the centre of the gaseous tritium target. The sample contained 0.737 mol of ^{232}Th nuclei.

The neutrons were recorded by a scintillation detector located at a distance of 198 cm from the centre of the sample. The detector, consisting of a stilbene crystal (diameter 6.3 cm, height 3.9 cm) in contact with an FEhU-30 photomultiplier, was placed in shielding whose design is described in Ref. [5]. The absolute efficiency of neutron recording by the detector in the range from recording threshold up to an energy of 11 MeV was determined by comparing the experimental and calculated prompt neutron spectra for spontaneous fission of ^{252}Cf . The calculated spectrum is described by a Maxwellian distribution with parameter $T = 1.42$ MeV; for the energy region above 6 MeV a correction was made to take account of the deviation of the ^{252}Cf fission neutron spectrum from a Maxwellian distribution [6]. The statistical error in the results of measuring the ^{252}Cf fission neutron spectrum was 2-7% and the time resolution of the spectrum was 3 ns at half-height of the gamma photon peak from the target. The width of the time analyser channel was 0.503 ns, the integral non-linearity 0.4% and the differential non-linearity 0.6%. To monitor the neutron flux we used a scintillation detector, which measured the time spectrum of the neutrons from the target. The yield of neutrons from the target was monitored also by an all-wave detector. The block diagram and the operating principle of the spectrometer electronics are set forth in Ref. [7].

Measurement of the neutron emission spectra from ^{232}Th was performed at angles of 90° and 150° at a neutron energy incident on the sample of 1.49 MeV. The investigations consisted of measurement of the spectra of the neutrons escaping from the sample (effect with background) and measurement of the background without the sample at a fixed number of protons incident on the target. At the same time the monitor was used to determine the spectrum of neutrons from the target. The measurements were carried out in groups in

order to reduce the influence of unstable operation of the accelerator and the electronic apparatus on the results. Stability of operation was checked by reference to the shape and position of the neutron peak in the monitor spectrum, and also to the position of the centre of gravity of the gamma-photon peaks in the monitor and principal detector spectra. Each series included measurement of the spectrum of neutrons escaping from the target at an angle of 0° in relation to the accelerated proton beam. The absolute value of the differential emission spectrum of neutrons from the ^{232}Th nuclei was determined by normalizing for the elastic scattering cross-section on carbon, measurement of which was carried out at an angle of 90° to the direction of the incident neutron beam. As scatterer we used a hollow cylinder of graphite (external diameter 3.0 cm, height 4.5 cm, thickness 0.5 cm), containing 14.27 mol of ^{12}C nuclei. The differential elastic scattering cross-section on carbon at an angle of 90° (in the laboratory system of co-ordinates), equal to 0.2033 b/sr, was taken from Ref. [8]. The recorded spectrum obtained in measurements with the ^{232}Th sample at an angle of 90° is shown in Fig. 1. After separation of the elastically scattered neutrons by the method explained in Ref. [9], the spectra were subjected to further processing in the energy range 2-10 MeV, which contained only neutrons formed upon fission. The method of treatment is described in detail in Ref. [10]. The prompt fission neutron energy spectra are given in Fig. 2.

Analysis of the shape of the ^{232}Th prompt fission neutron spectrum was carried out on the assumption that, for a sufficiently wide energy range, the spectrum is described by a Maxwellian distribution $N(E) = A \sqrt{E} \exp(-E/T)$. For selecting the distribution parameters A and T, conversion of the co-ordinates $N(E) \rightarrow \ln N(E)/\sqrt{E}$ in order to linearize the distribution curve was carried out. The experimental spectrum after conversion of the co-ordinates is shown in Fig. 3. Approximation of the experimental points by a Maxwellian distribution using the least-squares method in the energy range 2-10 MeV resulted in the values $A = 0.151 \pm 0.006 \text{ MeV}^{-3/2} \cdot \text{b}$,

$T = 1.27 \pm 0.04$ MeV. The assigned errors were calculated using the formulae from Ref. [11]. An analysis of the contribution of the various components to the total error is given in Ref. [10]. Integration of the normalized Maxwellian distribution with the parameters $A = 0.151 \text{ MeV}^{-3/2} \cdot \text{b}$ and $T = 1.27$ MeV within the energy range from zero to infinity gave a cross-section for emission of ^{232}Th nuclei fission neutrons of 0.185 ± 0.021 b, i.e.

$$\int_0^{\infty} 0.151\sqrt{E} \exp(-E/1.272) dE = \sigma_f(E_0) \bar{\nu}_p(E_0) = 0.185,$$

where $\sigma_f(E_0)$ is the cross-section for fission of ^{232}Th nuclei by 1.5 MeV neutrons, and $\bar{\nu}_p(E_0)$ is the mean number of prompt fission neutrons at this energy. On the other hand, using the recommended value $\sigma_f(1.5 \text{ MeV}) = 0.077$ b [12] and the experimental value $\bar{\nu}_p(1.5 \text{ MeV}) = 2.25$ [13], it is possible to get $\sigma_f \bar{\nu}_p = 0.1778$, which is in satisfactory agreement with the results of integrating the Maxwellian distribution describing the body of experimental points. In its turn, the value of the parameter T , calculated with reference to the ratio [14] $T = 2/3\bar{E} = 2/3 [0.74 + 0.35(\bar{\nu}_p + 1)]$, where \bar{E} is a mean Maxwellian distribution energy of 1.252 MeV, in good agreement with the value $T = 1.27 \pm 0.04$ MeV derived in the present work.

The angular dependence of the number of prompt fission neutrons is evaluated by comparing the number of neutrons escaping at angles of 90° and 150° . The ratio of the number of neutrons escaping at an angle of 150° to the number escaping at 90° is 1.04 ± 0.04 . The result obtained is in qualitative agreement with the data in Ref. [15], in which similar evaluations were carried out for ^{238}U prompt fission neutron spectra. The measured ^{232}Th prompt fission neutron spectrum is shown in the table.

The present work has yielded the following results:

1. The prompt neutron spectrum for fission of ^{232}Th in the energy range 2-10 MeV was measured. The data on ^{232}Th fission by

- 1.5 MeV neutrons have here been obtained for the first time. The total number of fission neutrons determined from the measured spectra is in good agreement with the values of σ_f and $\bar{\nu}_p$ as determined from the data in Refs [12, 13];
2. The experimental results show that it is possible satisfactorily to describe the spectrum in the 2-10 MeV energy region by a Maxwellian distribution with parameter $T = 1.27 \pm 0.04$ MeV;
 3. In the 7-10 MeV energy region there is some difference between the spectra measured at angles of 90° and 150° , but this difference lies within the limits of measurement error, which does not permit the drawing of conclusions regarding the angular dependence of ^{232}Th fission neutron spectra at the initial neutron energy concerned.

REFERENCES

- [1] Madland, D.G., Nix, J.R., Nucl. Sci. and Engng, Vol. 81 (1982) 213-271.
- [2] Blinov, M.V., Bojkov, G.S., Vitenko, V.A. In book: Neutron Physics: Proceedings of the 6th All-Union Conference on Neutron Physics, Kiev, 2-6 October 1983, Vol. 2, Moscow, TsNIIatominform (1984) 280-301 (in Russian).
- [3] WRENDA 83/84: Rep. INDC(SEC)-88/URSF. Vienna: IAEA (1983).
- [4] Fetisov, N.I., Simakov, S.P., Trufanov, A.M. et al. Prib. Tekh. Ekhsp., No. 6 (1980) 22-25 (in Russian).
- [5] Trufanov, A.M., Nesterenko, V.S., Fetisov, N.I. et al. ibid., No. 2 (1979) 50-55 (in Russian).
- [6] Grundl, J.A., Eisenhauer, C.M., In: Nucl. cross-sections and technol.: Proc. conf. 3-7 March, Washington, 1975, Vol. 1, NBS Special publ. 425 (1975) 250.
- [7] Simakov, S.P., Lovchikova, G.N., Trufanov, A.M. et al. At. Ehnerg., Vol. 51, No. 4 (1981) 244-247 (in Russian).
- [8] Nuclear standards file INDC/NEANDC. Version: 1980, INDC-36/LN. Vienna, (1981) A-9.
- [9] Simakov, S.P., Lovchikova, G.N., Trufanov, A.M. et al. Vopr. At. Nauk. i Tekh. Ser. Yad. Konst., No. 5(44) (1981) 23-26 (in Russian).
- [10] Lovchikova, G.N., Polyakov, A.V., Sal'nikov, O.A. et al. FEHI Preprint 1564, Obninsk (1984) (in Russian).

- [11] Hudson, D., Statistics for physicists, Moscow, Mir (1967) (in Russian).
- [12] Carlsson, A.D., Bhat, M.R., ENDF/B-V Cross-section measurement standards: BNL-NBS-51619 (1982).
- [13] Manilovskij, V.V., Vorob'eva, V.G., Kuz'minov, B.D. et al. At. Ehnerg., Vol. 54, No. 2 (1983) 83-86 (in Russian).
- [14] Howerton, R.J., Doyas, R.J., Nucl. Sci. and Engng, Vol. 46, N 3 (1971) 414-416.
- [15] Nair, S., Gayther, D.B., UK Nuclear data progress report: INDC(UK)-23/L. Harwell (1974) 26-28.

Paper received by editors on 22 January 1986.

Table. ^{232}Th prompt fission neutron spectrum.

E, MeV	$N_{\text{exp}}(E) \cdot 10^4,$ b/MeV	E, MeV	$N_{\text{exp}}(E) \cdot 10^4,$ b/MeV
2,03	6240 \pm 5,2	6,19	322 \pm 7
2,20	4531 \pm 5,2	6,36	266 \pm 7
2,40	3668 \pm 5,3	6,59	300 \pm 8,5
2,60	3214 \pm 5,3	6,84	231 \pm 8,5
2,81	2693 \pm 5,3	7,03	186 \pm 10
3,00	2648 \pm 5,3	7,23	226 \pm 10
3,19	2060 \pm 5,3	7,44	203 \pm 10
3,40	1901 \pm 5,6	7,59	175 \pm 12
3,60	1643 \pm 5,6	7,81	115 \pm 12
3,80	1549 \pm 5,6	8,05	121 \pm 12
3,99	1428 \pm 5,6	8,21	100 \pm 15
4,20	1125 \pm 5,6	8,38	92 \pm 15
4,42	1138 \pm 5,6	8,56	94 \pm 26
4,62	912 \pm 5,6	8,73	83 \pm 26
4,80	843 \pm 5,6	8,92	111 \pm 26
4,99	667 \pm 6,1	9,11	51 \pm 32
5,19	592 \pm 6,1	9,31	31 \pm 32
5,41	620 \pm 6,1	9,51	59 \pm 32
5,64	442 \pm 6,1	9,72	17 \pm 32
5,83	461 \pm 6,8	9,94	43 \pm 40
6,03	407 \pm 6,8	10,16	68 \pm 40

Note: 1. $N_{\text{exp}}(E) = 4\pi N_{\text{exp}}(E, 90^\circ)$.

2. The relative measurement error is shown in per cent.

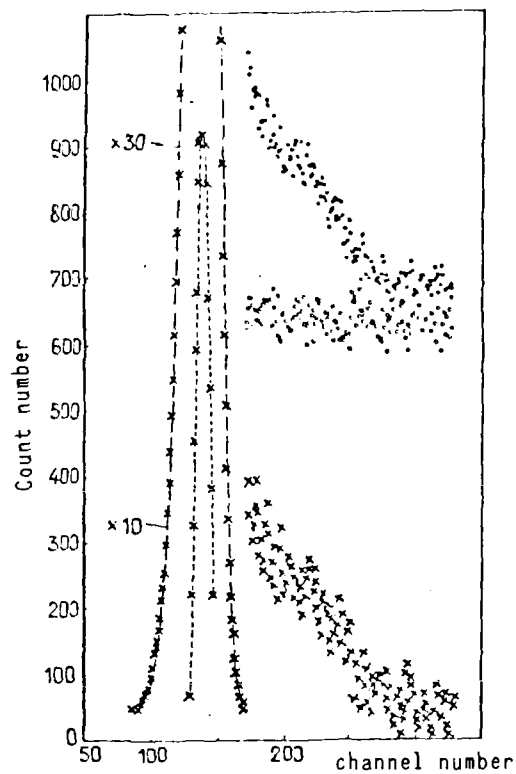


Fig. 1. Recorded spectra at an angle of 90°: ● - effect with background; ○ - background; X - effect.

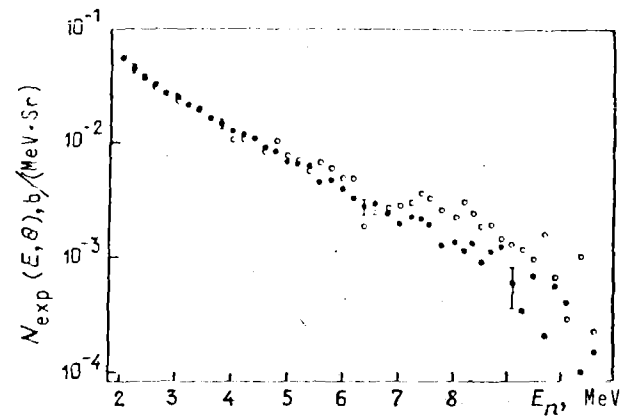


Fig. 2. Prompt fission neutron spectra at angles: ● - 90°; ○ - 150°.

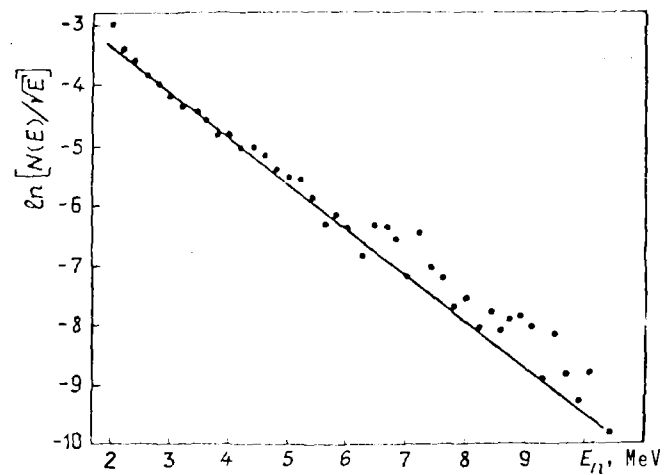


Fig. 3. Experimental spectrum (●) and its approximation by a Maxwellian distribution with parameter $T = 1.27$ MeV (straight line).

MEASUREMENT OF THE RADIATIVE NEUTRON CAPTURE CROSS-SECTION
FOR ^{238}U IN THE 4-460 keV ENERGY REGION

L.E. Kazakov, V.N. Kononov, G.N. Manturov, E.D. Poletaev
M.V. Bokhovko, V.M. Timokhov, A.A. Voevodskij

The radiative neutron capture cross-sections $\sigma_c(E)$ for ^{238}U in the 1-500 keV energy region is a highly important parameter used for calculations and optimization of fast breeder reactors. Demands are high with regard to the accuracy of this factor - 2-2.5% [1]. In recent years the cross-section $\sigma_c(E)$ for ^{238}U has been measured in various experimental facilities over a wide range of neutron energies [2-12]. However, the divergences in results have been significantly above the required accuracy level and for some energy ranges have been as high as 20-30%; this is due to the difficulty of measuring the radiative neutron capture cross-section for ^{238}U owing to the anomalous small neutron bonding energy, noticeable natural radiation background, strong neutron capture resonance self-shielding, and other factors.

The aim of the present paper is to obtain new experimental data on the neutron capture cross-section for ^{238}U for the 4-460 keV energy region. The measurement method and the experimental facility used differ significantly different from those in earlier work, and have enabled new results on the absolute value of the neutron capture cross-section for ^{238}U to be obtained.

Measurement method and experimental facility. The radiative neutron capture cross-section measurements were carried out in a fast and resonance neutron spectrometer using the EhG-1 pulsed Van-de-Graaff electrostatic accelerator at the Power Physics Institute (Obninsk) [13]. The measurements involved the registration of prompt capture gamma-quanta using a large liquid scintillation detector employing the time-of-flight method to determine neutron energy and for background discrimination. The saturated resonance method was used to normalize the cross-section; this method cuts out having

to measure the neutron source and the efficiency of the detector system directly.

The capture event detector comprised a spherical tank with a capacity of 17 L filled with a toluene-based scintillator with 60% trimethyl borate added. The neutron source was measured using a detector with a thin (1 mm thick) ^6Li window placed in front of the sample under investigation and a detector consisting of a ^{10}B plate and 2 NaI(Tl) crystals which was placed behind the sample.

The experiment was carried out in three stages:

- Measurements in the 2-130 keV region with a path length of 0.72 m;
- Measurements in the 30-460 keV neutron energy region with a path length of 2.4 m;
- Measurements in the resonance region with a path length of 2.4 m.

The spectrometer parameters for the experiments are given in Table 1.

A metallic lithium target was used to generate neutrons via the reaction $^7\text{Li}(p,n)^7\text{Be}$. In the last experiment, to obtain resonance neutrons the target was surrounded by a polyethylene moderator the dimensions of which were chosen with a view to optimizing resonance neutron yield and the spectrometer resolution required to observe the "shelves" of the ^{238}U saturated resonance at $E_0 = 6.67$ eV. The geometry for all three experiments and the parameters of the electronic apparatus (amplification and discrimination thresholds) remained the same. The neutron beam was collimated in such a way that its diameter did not exceed the diameter of the sample and the diameter of the neutron beam detectors. The shape and position of the neutron beam on the sample were monitored by means of special experiments with ring samples made of metallic indium. A detailed description of the experimental apparatus, the electronic apparatus and the measurement procedure is given in Refs [14-16]. A lot of attention was paid in the experiment to reducing the level of capture event detector background; this background can

be divided provisionally into a constant component (independent of the flight time) and a variable (prompt) component.

The constant background is caused by cosmic radiation, natural radioactivity, and additional background in the building due to the neutron beam and operation of the accelerator. This background, which is the main component of the general background, was significantly reduced during measurements with a flight path of 2.4 m by placing the detector system in an insulated area separated from the accelerator target hall by a two-metre wall of heavy concrete, and by the use of lead shielding. In experiments with a short flight path, when the detector system was situated in the target hall, the target was surrounded by a compact shield comprising a mixture of LiH and paraffin to reduce the neutron background, and a 150 mm thick lead shielding wall was placed between the detector and the target. Thus, despite an increase in the background from the liquid scintillation detector, thanks to the short path used in these measurements a significantly improved effect-to-background ratio (better by a factor of approximately 10) was achieved by comparison with the experiments with a flight path of 2.4 m. In the course of each irradiation the constant background level was measured to a high degree of accuracy ($\sim 0.5\%$) for the portion of the spectrum between the gamma peak and the moment where neutrons of maximum energy were registered for measurements with a long flight path, and in the region of the $E_0 = 2.85$ keV resonance of the ^3Na filter which was constantly fixed on the neutron beam for measurements with a short path, and in the region of the $E_0 = 3.86$ and 9.15 eV resonances of the ^{115}In filter which was constantly in position for measurements in the resonance region.

In experiments with a short flight path, in spectra measured by time of flight, a variable background component was observed which was related to the registration of instances of source neutron capture in the shielding, the lifetime of these neutrons being 150–200 ns in such systems. This component comprised 5–10% of the effect and was measured in experiments with no sample.

The prompt background is caused by the registration of beam neutrons scattered in the sample under investigation and, together with the constant neutron background, it was reduced by adding trimethyl borate to the scintillator. Special research carried out with graphite and ^{208}Pb scatterers showed that the sensitivity of our detector to scattered neutrons was no greater than 7×10^{-3} at 5 keV, and it went down to 2×10^{-5} at 100 keV. Under experimental conditions the prompt component of the background comprised 2-10% of the effect and was measured in experiments with an equivalent scatterer.

Another important source of systematic errors in experiments measuring capture cross-sections is the finite thickness of the samples used. In order to uncover these errors and to check whether the relevant corrections had been properly introduced, measurements were carried out with a metallic sample and oxide samples of two thicknesses. Samples prepared from depleted ^{238}U containing less than 0.004% ^{235}U were packed in aluminium containers with a diameter of 40 mm and a wall thickness of 0.07 mm (Table 2).

During the experiment, the radiative capture cross-section for ^{197}Au was measured as well as that for ^{238}U . The measurement results helped monitor experimental conditions, and produced independent data on the absolute value of the ratio of these two cross-sections.

Normalization of cross-section and corrections. Using the saturated resonance method for normalization, the radiative neutron capture cross-section can be obtained as follows:

$$\sigma_c(E) = K \frac{N_c(E)}{N_{\text{Li}}(E)} \frac{1}{n} \frac{\sigma_{n\alpha}(E)}{\sigma_{n\alpha}^2} \frac{S_{\text{Li}}(E)}{S(E)T_{\text{Li}}(E)}, \quad (1)$$

where K is the normalization coefficient; $N_c(E)$ and $N_{\text{Li}}(E)$ are the number of counts from the capture event detector and the neutron source detector with the ^6Li window in the fast neutron region in relation to energy; N is the number of nuclei in the sample under investigation, atoms/b; $\sigma_{n\alpha}(E)$, $\sigma_{n\alpha}^r$ is

the cross-section of the reaction ${}^6\text{Li}(n,\alpha){}^3\text{H}$ for a neutron energy E in the saturated resonance region; $S_{\text{Li}}(E)$ is the correction for resonance self-shielding and multiple scattering of neutrons in the sample; $T_{\text{Li}}(E)$ is the transmission of the detector with the ${}^6\text{Li}$ window. The coefficient K was determined from measurements in the saturated resonance region using the function

$$K = \frac{N_{\text{Li}}^z}{N_{\text{C}}^z} P_{\text{C}}^z \frac{T_{\text{Li}}^z}{S_{\text{Li}}^z} \frac{F_{\gamma}^z \epsilon_{\gamma}^z}{F_{\gamma}^f \epsilon_{\gamma}^f}, \quad (2)$$

where the index r denotes values in the saturated resonance region; f denotes the same in the fast neutron region; P_{C}^r is the probability of radiative capture of neutrons in the sample; F_{γ} is the correction for self-absorption of capture gamma quanta in the sample; ϵ_{γ} is the efficiency of the capture event detector.

The probability of neutron capture in the sample in the saturated resonance region P_{C}^r was determined from known resonance parameters taking into account contribution from nearby resonances and the multiple neutron scattering effect which was calculated using the Monte Carlo method. For the sample of metallic uranium used in the measurements in the resonance region a probability P_{C}^r of 0.99 ± 0.02 was obtained ($E_0 = 6.67$ eV), and for the gold sample - 0.98 ± 0.02 ($E_0 = 4.9$ eV). The error level in the calculation of P_{C}^r is mainly due to uncertainty regarding the widths Γ_n and Γ_{γ} for these resonances.

The ratio $(F_{\gamma}^r \epsilon_{\gamma}^r) / (F_{\gamma}^f \epsilon_{\gamma}^f) = 1 \pm 0.02$ both for ${}^{238}\text{U}$ and for gold was obtained by analysing the capture event spectra in the fast and resonance regions and calculating the correction for self-absorption of capture gamma quanta in the sample which was done by the Monte Carlo method using the BRAND program package [17].

When calculating the correction F_{γ} , model spectra were used representing a series of gamma quanta cascades [18] corresponding to

experimental thermal neutron capture gamma spectra both in shape and average number. A typical value for the correction F_{γ} for the samples used was 0.9–0.95, but for the ratio $F_{\gamma}^F/F_{\gamma}^f$ a value of 0.98 ± 0.01 was obtained. This ratio diverges from unity owing to the varying distribution of fast and resonance neutron capture events over the sample thickness.

The efficiency ratio $\epsilon_{\gamma}^F/\epsilon_{\gamma}^f = 1.02 \pm 0.02$ was obtained by comparing the count above the registration threshold measured in the fast and resonance neutron region. Capture events were reduced to an identical number by normalizing to the total gamma quanta energy obtained by the amplitude weighting method using the weighting function for our detector [19]. The result was confirmed by comparing the shape of capture event amplitude spectra normalized by area; these do not change as they pass from the saturated resonance to the fast neutron region within the limits of statistical accuracy ($\pm 2\%$).

Thus, taking into account uncertainties regarding the introduction of other insignificant corrections (T_{Li}^F and S_{Li}^F) which form part of expression (2), and doubts concerning the measurable experimental ratio N_{Li}^F/N_c^F , the accuracy of the normalization method was judged to be $\pm 3\%$.

The relative behaviour of the ${}^6\text{Li}(n,\alpha){}^3\text{H}$ reaction cross-section was used to obtain the cross-section $\sigma_c(E)$ up to 130 keV. For higher energies the reaction ${}^{10}\text{B}(n,\alpha\gamma){}^7\text{Li}$ was used to determine neutron flux shape and the data were normalized to obtain absolute values for the cross-section in the 50–100 keV range. The evaluation for the cross-sections of these reference reactions given in the ENDF/B-V library was used [20].

The correction for multiple scattering of neutrons in neutron flux detectors was calculated using the Monte Carlo method and the BRAND program package. For the detector with the ${}^6\text{Li}$ window the correction was 4–4.5% in the 4–130 keV energy range, and for the detector with the ${}^{10}\text{B}$ plate the correction ranged from 13% at $E_n = 30$ keV to 16% at $E_n = 450$ keV. It

should be noted that, since the data obtained in relation to the $^{10}\text{B}(n,\alpha\gamma)^7\text{Li}$ reaction were normalized to results obtained in relation to the $^7\text{Li}(n,\alpha)^3\text{H}$ reaction, the uncertainty with regard to the introduction of this correction for the detector with the ^{10}B plate depends not on its absolute value but its energy dependence.

The methodology put forward in Ref. [21] was used to calculate the correction for resonance self-shielding and multiple scattering of neutrons in the samples used. The correction amounted to 1% at a neutron energy of 4 keV and increased smoothly up to 7% for higher energy levels. The main source of uncertainty with regard to calculation of this correction is the error level of the resonance parameters and it is evaluated at 2%.

It should be noted that the inference above that the value $F_{\gamma\epsilon_{\gamma}}$ changes but little when moving from the saturated resonance to the fast region allows one to determine the absolute value of the capture event detector efficiency ratio for uranium and gold from measurements in the resonance region, and thus to obtain the $\sigma_c^{\text{U}}(E)/\sigma_c^{\text{Au}}(E)$ cross-section ratio. This functional would seem to be an important additional piece of information in that it is independent of the reference cross-sections of the $^6\text{Li}(n,\alpha)^3\text{H}$ and $^{10}\text{B}(n,\alpha\gamma)^7\text{Li}$ reactions and thus avoids the inherent uncertainties of the latter.

Results and comments. The results of the neutron capture cross-section measurements are given in Table 3. Columns 1 and 2 contain the results obtained for a sample of metallic uranium in relation to the cross-sections of the reference reactions $^6\text{Li}(n,\alpha)^3\text{H}$ and $^{10}\text{B}(n,\alpha\gamma)^7\text{Li}$ respectively, and columns 3 and 4 contain the results for an oxide sample of thickness 0.00654 atoms/b.

Analysis of the data obtained from measurements with different types of sample showed that, after the relevant corrections for the finite thickness of the samples have been introduced, the measurements agree within the limits of evaluable error. Therefore, the final values of $\sigma_c(E)$ for ^{238}U were

obtained by averaging the results of all the different measurements with the weight which is inversely proportional to the square of the error level.

The measurement error level comprises the statistical accuracy which was defined as the mean square spread between series (from 6 to 21 for the different types of sample), the error level for eliminating the background, the normalization error level, uncertainty in the relative behaviour of the reference cross-sections, the error level for the introduction of corrections. The components of the total error level in relation to neutron energy are given in Table 4.

The figure compares the results obtained on $\sigma_c(E)$ for ^{238}U with the data from other papers. One can see that there is a high level of agreement with the data from Ref. [2], especially for the 10-100 keV energy range where results agree to $\pm 3\%$ with the exception of two points (at 35 and 85 keV). In the 4-10 keV energy region the data from Ref. [2] are lower than our results by 10% on average. In the 4-30 keV energy region our results tally with those in Ref. [8], whereas the data from Ref. [3] are approximately 30% lower. It should be noted that in this energy region, owing to the low level density, the capture cross-section can fluctuate a lot. Therefore, the different averaging intervals used in the various papers can be an additional cause for divergence of results. The data from Ref. [4] show a fair level of agreement with our results for energies below 10 keV, but in the 20-100 keV region they are systematically higher by 15%. In the 30-300 keV energy region there is a high level of agreement for the absolute value with the last data from Ref. [12].

Comparing the results obtained with the results of other authors one comes to the conclusion that, in the 10-200 keV energy region, they lie on the lower limit of all the experimental data. We note also that our data show a high level of agreement over the whole neutron energy range investigated with the latest evaluation given in Ref. [22] which was based on a simultaneous analysis of the experimental data on all neutron cross-sections for ^{238}U .

The results obtained show clearly the sharp change in the energy dependence of $\sigma_c(E)$ above 44.7 keV which is caused by the opening up of the inelastic neutron scattering channel with excitation of the first 2^+ level in ^{238}U . There are striking fluctuations in the capture cross-section in the 150-300 keV energy region; they appear in other papers too [7, 12]. However, the detailed behaviour of these fluctuations cannot be taken to be reliably confirmed at present and it is entirely possible that they are caused by systematic measurement errors not taken into consideration.

The experimental results obtained on the neutron capture cross-section were analysed within the framework of the statistical theory of nuclear reactions in order to determine mean resonance parameters. For this analysis, the EVPAR program was used [23] in which the radiative neutron capture cross-section is calculated using the Hauser-Feshbach-Moldauer model and the theoretical cross-section curve optimized with the experiment using the maximum likelihood method. The program was also used to set up a correlation matrix for error levels in the experimental data based on the above analysis of the components of the total error level in the measurements.

Above 10 keV the contribution of neutrons with non-zero orbital momentum to the capture cross-section becomes significant and, consequently, the value of the cross-section in the energy range studied is determined using s-, p- and a-wave neutron and radiation strength functions. To reduce the number of variable parameters, the s-wave neutron strength function was taken to be equal to $S_0 = 1.11 \times 10^{-4}$ ($\pm 10\%$), which value was obtained from an analysis of resolved resonances in Ref. [24] to a high level of reliability.

By analysing the data below 10 keV where the capture cross-section is determined in the main by the s-wave, a value for the radiation strength function $S_{\gamma 0}$ was obtained which, within evaluable error limits ($\pm 10\%$), coincided with the resonance value. Therefore, in subsequent analysis, $S_{\gamma 0}$ was assumed to be equal to the resonance value $S_{\gamma 0} = 11.3$ ($\pm 4\%$) given in Ref. [24] and was not varied.

The optimal values of the mean resonance parameters, including the values for the four strength functions S_1 , S_2 , $S_{\gamma 1}$ and $S_{\gamma 2}$ found by us, and their correlation matrix, are given in Table 5. Generation of the correlation matrix takes into account the error levels for S_0 and $S_{\gamma 0}$ taken from the resolved resonance region.

The values obtained for the neutron and radiation strength functions for p- and d-neutrons did not differ significantly from the parameters given in Ref. [22], although some of the starting positions were different. Overall, our data on the neutron capture cross-section in ^{238}U over the whole 4-460 keV energy range fit in well with the Hauser-Feshbach-Moldauer model using the resonance values for S_0 and $S_{\gamma 0}$. At the same time, the values for the radiation strength functions for s- and d-neutrons are close to one another, but for p-neutrons they are 25% lower.

* * *

Several cycles of measurements were performed yielding new experimental data on the value of the radiative neutron capture cross-section for ^{238}U in the 4-460 keV energy region. The accuracy level of the results in the 10-460 keV energy region is 4.5-6.0%. In this energy region the data obtained lie on the lower limit of all the experimental results, but they show a high level of agreement with the latest evaluation of the capture cross-section done by the Power Physics Institute and incorporated in the FOND evaluated data library [25]. The capture cross-section was analysed using the Hauser-Feshbach-Moldauer model and this showed that the data obtained agreed well with theoretical calculations using the resonance values for S_0 and $S_{\gamma 0}$.

REFERENCES

- [1] WRENDA: World request list for nuclear data: 83/84, INDC(SEC) 88/URSF, IAEA, Vienna (1983).
- [2] MOXON, M.C. The neutron capture cross-section of ^{238}U in the energy region 0.5 to 100 keV, AERE-R6074, UK Atomic Energy Authority (1969).

- [3] FRICKE, M.P., MATHEWS, D.R., FRIESENHAHN, S.J., et al., Proc. conf. neutron cross-section technol. 1 (1971) 252.
- [4] DE SAUSSURE G., SILVER, E.G., PEREZ, R.B., et al., Measurement of the uranium-238 capture cross-section for incident neutron energy up to 100 keV, Nucl. Sci. and Engng. 51 (1973) 385, 404.
- [5] SPENCER, R.R., KAEPPELER, F., Measurement of the ^{238}U capture cross-section shape in the neutron energy region 20 to 550 keV, in Nucl. cross-section and technol. (Proc. of Intern. conf. Washington) 2 (1975) 620, 622.
- [6] PANITKIN, Yu.G., SHERMAN, L.E., Absolute measurements of the radiative capture cross-section for 30 keV neutrons in ^{238}U , At. Ehnerg. 39, 1, (1975) 17, 19 [in Russian].
- [7] LE RIGOLEUR, C., ARNAUD, A., TAST, J., Absolute measurements of neutron radiative capture cross-sections for ^{23}Na , Cr, ^{55}Mn , Fe, Ni, ^{103}Rh , Ta, ^{238}U in the keV energy range, in [5] 953, 956.
- [8] ADAMCHUK, Yu.V., VOSKANYAN, M.A., MURADYAN, G.V., et al., Measurement of the capture cross-section for uranium-238, in Neutron Physics (Proc. 4th All-Union Conference on Neutron Physics, Kiev, 18-22 April 1977), Part 1, TsNIIatominform, Moscow (1977) 192, 195 [in Russian].
- [9] WISSHAK, K., KAEPPELER, F., Neutron capture cross-section ratios of ^{240}Pu , ^{242}Pu , ^{238}U and ^{197}Au in the energy range from 10 to 90 keV, Nucl. Sci. and Engng. 66 (1978) 363, 377.
- [10] DAVLETSHIN, A.N., TIPUNKOV, A.O., TIKHONOV, S.V., TOLSTIKOV, V.A., Measurement of the radiative neutron capture cross-sections for ^{238}U and ^{197}Au in relation to the inelastic scattering cross-section for neutrons against protons, At. Ehnerg. 48 2 (1980) 87, 91 [in Russian].
- [11] YAMAMURO, N., SAITO, K., EMOTO, T., et al., Neutron capture cross-section measurements of ^{93}Nb , ^{127}I , ^{165}Ho , ^{181}Ta and ^{238}U between 3.2 and 80 keV, J. Nucl. Sci. and Technol. 17 (1980) 582-592.
- [12] POENITZ, W.P., Measurements of the neutron capture cross-section of gold-197 and uranium-238 between 20 and 3500 keV, Nucl. Sci. and Engng. 57 (1975) 300, 308; POENITZ, W.P., FAWCETT, L.R. Jr., and SMITH D.L., Measurements of the $^{238}\text{U}(n,\gamma)$ cross-section at thermal and fast energies, *ibid.* 78 (1981) 239-247.
- [13] KONONOV, V.N., POLETAEV, E.D., BOKHOVKO, M.V., et al., A fast and resonance neutron spectrometer using the EhG-1 electrostatic accelerator, Vopr. at. nauki i tekhniki, Ser. Yad. konstanty 1 (40) (1981) 67 [in Russian].
- [14] KONONOV, V.N., POLETAEV, E.D., BOKHOVKO, M.V., et al., Absolute measurement method for the radiative fast neutron capture cross-section in uranium-238, in Neutron Physics (Proc. 5th All-Union Conference on Neutron Physics, Kiev, 15-19 September 1980), Part 2, TsNIIatominform, Moscow (1980) 280 [in Russian].
- [15] KAZAKOV, L.E., KONONOV, V.N., POLETAEV, E.D., et al., Measurement of the radiative neutron capture cross-sections for ^{236}U and ^{197}Au in the 3-420 keV energy region, Vopr. at. nauki i tekhniki, Ser. Yad. konstanty 2 (1985) 44, 49 [in Russian].

- [16] BOKHOVKO, M.V., KAZAKOV, L.E., KONONOV, V.N., et al., Spectrometric apparatus for absolute measurement of the radiative fast neutron capture cross-section in uranium-238, Preprint FEhI-973 [Power Physics Institute], Obninsk (1979) [in Russian].
- [17] ANDROSENKO, A.A., ANDROSENKO, P.A., The BRAND program package for calculating radiation transfer characteristics using the Monte Carlo method, Vopr. at. nauki i tekhniki, Ser. fizika i tekhnika yadernykh reaktorov 7 (1985) 33, 37 [in Russian].
- [18] ANDROSENKO, P.A., BOLONKINA, G.V., KONONOV, V.N., et al., Calculation of the response function for a large scintillation detector for neutron capture events using the Monte Carlo method, Preprint FEhI-1604, Obninsk (1984) [in Russian].
- [19] KONONOV, V.N., POLETAEV, E.D., TIMOKHOV, V.M., et al., Use of the amplitude weighting method for a large scintillation detector, Preprint FEhI-1589, Obninsk (1984) [in Russian].
- [20] Nuclear Standards File 1980 version, INDC-36/LM, IAEA, Vienna (1981).
- [21] MACKLIN, R.L., Resonance self-shielding in neutron capture cross-section measurements, Nucl. Instrum. and Methods 26 (1964) 213, 15.
- [22] MANTUROV, G.N., LUNEV, V.P., GORBACHEVA, L.V., Evaluation of neutron data for ^{232}Th and ^{238}U in the unresolved resonance region, in Neutron Physics (Proc. 6th All-Union Conference on Neutron Physics, Kiev, 2-6 October 1983), Vol. 2, TsNIIatominform, Moscow (1983) 231, 237 [in Russian].
- [23] MANTUROV, G.N., LUNEV, V.P., GORBACHEVA, L.V., Evaluation of neutron data for ^{232}Th in the unresolved resonance region, Vopr. at. nauki i tekhniki, Ser. Yad. konstanty 1 (1983) 50, 63 [in Russian].
- [24] NIKOLAEV, M.N., ABAGYAN, L.P., KORCHAGINA, Zh.A., et al., Neutron data for uranium-238: analytical review, Part 1, Obninsk (1978) [in Russian].
- [25] KOSHCHEEV, V.N., NIKOLAEV, M.N., Neutron data library for the calculation of group constants, Vopr. at. nauki i tekhniki, Ser. Yad. konstanty 5 (1984) 16, 20 [in Russian].

Submitted for publication 3 February 1986.

Table 1

Neutron spectrometer parameters

Parameter	Experiment		
	1	2	3
Van-de-Graaff accelerator			
Energy:			
Protons, MeV	1,9	2,1	2,8
Neutrons, keV	2-130	30-460	1-30 eV
Pulse length, ns	4	5	0,4 μ s
Repetition interval, μ s	1,7	2,2	140
Mean current, μ A	2	1,8	1,5
Spectrometer flight path, m:			
Large liquid scintillation detector	0,72	2,4	2,4
Detector:			
with ^6Li window	0,51	2,2	2,2
with ^{10}B plate	-	2,7	-

Table 2

Characteristics of samples used

Sample No.	Sample	Thickness, atoms/b
1	^{238}U (metallic)	0,00646
2	$^{238}\text{U}_3\text{O}_8$	0,00654
3	$^{238}\text{U}_3\text{O}_8$	0,00274
4	^{197}Au	0,00458
5	^{197}Au	0,00229

Table 3

Measurement results for the neutron capture cross-section for ^{238}U and ratios of the neutron capture cross-sections in ^{238}U and ^{197}Au

E_n , keV	σ_c , nb				$\langle \sigma_c \rangle$, nb	$R = \sigma_c^{\text{U}} / \sigma_c^{\text{Au}}$
	1	2	3	4		
4-5	1018	-	1290	-	1154 \pm 192	0,530 \pm 0,094
5-6	1085	-	1225	-	1155 \pm 158	0,572 \pm 0,084
6-7	881	-	880	-	881 \pm 97	0,509 \pm 0,061
7-8	819	-	880	-	850 \pm 80	0,584 \pm 0,059
8-9	713	-	820	-	767 \pm 61	0,566 \pm 0,049
9-10	668	-	808	-	738 \pm 52	0,621 \pm 0,051
10-12	643	-	719	-	681 \pm 42	0,582 \pm 0,044
12-14	653	-	707	-	680 \pm 38	0,689 \pm 0,044
14-16	584	-	598	-	589 \pm 31	0,714 \pm 0,043
16-18	572	-	594	-	583 \pm 29	0,727 \pm 0,042

Table 3 (continued)

E_n keV	σ_c , nb				$\langle \sigma_c \rangle$, nb	$R = \sigma_c^U / \sigma_c^{All}$
	1	2	3	4		
18-20	530	-	569	-	550+27	0,776+0,044
20-22	514	-	535	-	525+25	0,763+0,043
22-24	480	-	491	-	486+23	0,788+0,044
24-26	458	-	486	-	472+22	0,752+0,041
26-28	455	-	469	-	462+21	0,769+0,042
28-30	437	-	473	-	455+21	0,733+0,041
30-35	428	419	440	440	434+20	0,785+0,044
35-40	400	403	407	409	405+18	0,770+0,042
40-45	381	376	387	371	384+17	0,820+0,044
45-50	333	316	336	341	335+15	0,748+0,040
50-55	287	301	298	303	294+13	0,721+0,039
55-60	272	292	280	278	277+12	0,692+0,037
60-65	256	263	262	264	260+12	0,664+0,037
65-70	237	254	240	226	240+11	0,627+0,035
70-75	222	234	230	221	226+10	0,613+0,033
75-80	216	224	218	214	217+9,8	0,605+0,033
80-85	208	195	204	208	207+9,3	0,597+0,033
85-90	199	194	198	201	200+9	0,602+0,033
90-95	187	195	192	194	191+8,6	0,590+0,032
95-100	182	187	186	181	184+8,3	0,579+0,032
100-110	182	175	186	169	184+8,3	0,571+0,031
110-120	173	169	172	161	173+7,8	0,585+0,032
120-130	168	165	162	163	164+9,5	0,575+0,038
130-140	-	155	-	147	151+8,8	0,534+0,035
140-150	-	152	-	142	147+8,5	0,531+0,035
150-160	-	138	-	139	138+8,1	0,493+0,032
160-170	-	144	-	139	142+8,1	0,515+0,033
170-180	-	136	-	139	138+7,9	0,509+0,033
180-190	-	140	-	133	137+7,8	0,515+0,033
190-200	-	145	-	135	140+7,8	0,539+0,034
200-210	-	144	-	133	139+7,8	0,533+0,034
210-220	-	137	-	134	136+7,6	0,506+0,032
220-230	-	137	-	130	134+7,4	0,498+0,031
230-240	-	136	-	129	133+7,3	0,516+0,032
240-250	-	126	-	121	124+6,8	0,481+0,030
250-260	-	132	-	117	125+6,9	0,500+0,032
260-270	-	123	-	122	122,5+6,7	0,492+0,031
270-280	-	132	-	119	126+6,8	0,510+0,032
280-290	-	141	-	125	133+7,2	0,613+0,038
290-300	-	132	-	133	132,5+7,2	0,634+0,040
300-320	-	135	-	127	131+6,9	0,642+0,039
320-340	-	138	-	122	130+6,9	0,688+0,042
340-360	-	130	-	124	127+6,6	0,726+0,044
360-380	-	127	-	122	125+6,5	0,767+0,046
380-400	-	126	-	120	123+6,3	0,794+0,047
400-420	-	124	-	118	121+6,1	0,801+0,047
420-440	-	121	-	121	121+6,1	-
440-460	-	126	-	122	124+6,1	-

Note: Capture cross-sections in relation to the reactions: 1 - ${}^6\text{Li}(n,\alpha){}^3\text{H}$ (metal); 2 - ${}^{10}\text{B}(n,\alpha\gamma){}^7\text{Li}$ (metal); 3 - ${}^6\text{Li}(n,\alpha){}^3\text{H}({}^{238}\text{U}_3\text{O}_8)$; 4 - ${}^{10}\text{B}(n,\alpha\gamma){}^7\text{Li}({}^{238}\text{U}_3\text{O}_8)$.

Table 4

Error levels of experimental results

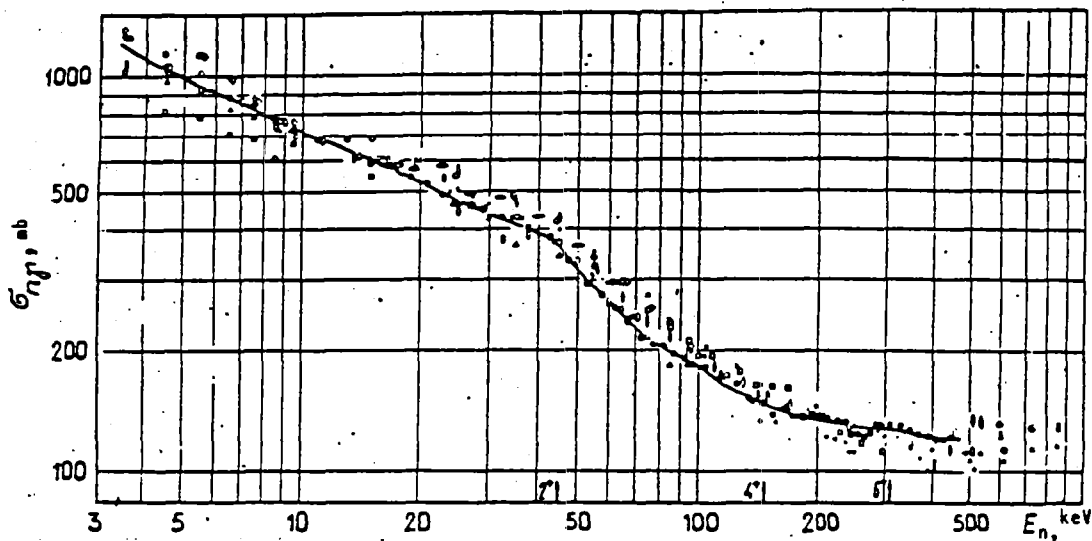
E_n , keV	Error level				E_n , keV	Error level			
	Statistical	Elimination of background	Reference reaction cross-sections	Total		Statistical	Elimination of background	Reference reaction cross-sections	Total
4-5	10,6	12,2	0,5	16,6	120-130	3,8	0,5	2,0	5,6
5-6	7,2	11,0	0,5	13,7	200-210	3,8	0,5	1,6	5,7
0-12	3,0	3,4	1,0	6,1	300-320	3,0	0,5	2,0	5,3
0-35	0,7	0,5	2,0	4,5	440-460	2,2	0,5	2,0	4,5
0-120	0,65	0,5	2,0	4,5					

Note: For all energy values the normalization error is 3.0%, and the error level for the introduction of corrections 2.5%.

Table 5

Optimum values for the mean resonance parameters for ^{238}U and comparison with the evaluation in Ref. [22]

Parameter	Optimum value, $\times 10^{-4}$	Error level, %	Correlation coefficients						Evaluation in Ref. [22] $\times 10^{-4}$
			S_0	S_1	S_2	S_{δ_0}	S_{δ_1}	S_{δ_2}	
S_0	1,11 [24]	10,0	I						0,93 \pm 0,03
S_1	2,2	8,5	-0,16	I					2,30 \pm 0,07
S_2	2,8	9,7	0,03	0,03	I				3,0 \pm 0,3
S_{δ_0}	11,3 [24]	4,0	-0,08	-0,55	0,02	I			11,0 \pm 0,3
S_{δ_1}	8,1	6,5	0,27	0,03	-0,01	-0,21	I		8,0 \pm 0,3
S_{δ_2}	10,8	10,4	0,52	0,31	-0,37	-0,18	-0,14	I	8,0 \pm 0,3



Radiative capture cross-section for ^{238}U . Sources of data: ● - Present work; ◊ - [4]; ○ - [5]; × - [6]; + - [7]; ◊ - [8]; ○ - [9]; ⊕ - [10]; □ - [11]; □ - [12]; the curve represents the results of the authors' calculation using the EYPAR program with the parameters from Table 5.

EVALUATION OF MEAN RESONANCE PARAMETERS FOR ^{235}U , PLUTONIUM ISOTOPES
AND ^{241}Am USING DATA FROM THE RESOLVED RESONANCE REGION

V.A. Kon'shin, N.K. Salyakhov

Reference [1] examines the basic principles employed in analytical methods for evaluating mean resonance parameters: Δ_3 -statistics [2], moments [3], maximum likelihood taking into account omission of weak resonances [4, 5], and the maximum likelihood method taking into account omission of weak resonances and omission of resonances owing to multiplicity [6, 7]. In Ref. [1], only the best methods [4, 6] for analysing data on ^{238}U were described and used. This paper presents an example of the joint use of the above methods to evaluate mean parameters for ^{235}U , plutonium isotopes and ^{241}Am .

In the Δ_3 -statistics method [2], the region where there is no resonance omission is determined on the basis of the assumption that the true resonance density is not dependent on energy. In other words, it is assumed that the dependence of the rising sum of resonances $N(E)$ on energy is linear in the region where there is no omission. This region may be defined using the following condition [3]

$$\langle \Delta_3(E) \rangle - \sigma(\Delta_3) \leq \Delta_3(E) \leq \langle \Delta_3(E) \rangle + \sigma(\Delta_3),$$

where

$$\Delta_3(E) = \min_{A,B} \int_{\Delta E} [N(E) - (AE + B)]^2 dE; \quad \langle \Delta_3(E) \rangle = 1/\pi^2 \left\{ \ln [N(E) - 0,0687] \right\}; \quad \sigma^2(\Delta_3) = 0,012.$$

The moments method [3] uses neutron width distribution moments to take account of weak resonance omission. It is assumed that all resonances whose reduced widths $g\Gamma_n^0$ are greater than the conditional proportion α of the true mean $\langle g\Gamma_n^0 \rangle$ are detected. In essence, the method compares the expected theoretical value for the factor derived from the distribution moments for α with the experimental value over the number of widths n_α for which $g\Gamma_n^0 \geq \alpha \langle g\Gamma_n^0 \rangle$ [4]:

$$n_{\alpha} \frac{\sum_{>\alpha <g\Gamma_n^0>}^{n_{\alpha}} g\Gamma_n^0}{\left[\sum_{>\alpha <g\Gamma_n^0>}^{n_{\alpha}} \sqrt{g\Gamma_n^0} \right]^2} = \frac{\int_{\alpha}^{\infty} x f(x) dx \int_{\alpha}^{\infty} f(x) dx}{\left[\int_{\alpha}^{\infty} \sqrt{x} f(x) dx \right]^2}, \quad (1)$$

where

$$f(x) dx = (2\pi x)^{-1/2} \exp(-x) dx; \quad x = g\Gamma_n^0 / 2 <g\Gamma_n^0> .$$

The summations in the left-hand portion of the equation are calculated by decreasing the widths until the ratio given in expression (1) is achieved, and $F(\alpha) = \int_{\alpha}^{\infty} f(x) dx$ determines what proportion of the true number N of resonances in the set is comprised by n_{α} . The authors of Ref. [3] used only one value of $\alpha = 0.24$ in this method. Clearly, the non-dependence of the result on α would be proof of the evaluation of N is reliable, and therefore it would be useful to study the dependence $N(\alpha)$.

Coceva's maximum likelihood method can be used to determine the mean reduced neutron width $\langle g\Gamma_n^1 \rangle$ for p-resonances as well as the parameters $\langle g\Gamma_n^0 \rangle$ and $\langle D \rangle_0$ (mean distance for s-resonances). The choice of the shape and height of the conditional threshold $\eta(E)$ above which it is assumed there is no omission of resonances is an important feature of the use of this method [4]. We have used the type of threshold proposed in Ref. [5]:

$$\eta(E) = (AE^B + C)t, \quad (2)$$

where t is a variable parameter; the coefficients A, B, C are selected for $t = 1$ on the basis of correspondence to the real resonance registration threshold.

The Fröhner method [6] can be used to take into account diffuseness of the real resonance registration threshold. The parameters for the conditional threshold, which is not set in any manifest way, are selected automatically. The weakness of this method is the way it approximates the curve for the rising sum of resonances when obtaining the expression for observable resonance density. In some instances, the lack of similarity to the

likelihood function owing to the incorrect approximation prevented us from using this method to analyse ^{241}Pu data.

The above-mentioned methods vary with respect to their reliability.

Six factors which affect reliability may be singled out:

1. Allowance for the energy dependence of the threshold above which all resonances are determined experimentally;
2. Allowance for diffuseness of the real registration threshold;
3. Allowance for omission of resonances owing to the multiplicity of observable peaks;
4. Use of data on the energy dependence of the density of observable peaks;
5. Use of data on neutron width distribution;
6. Use of data on the distribution of the distances between resonances.

Table 1 shows which of these factors each of the various methods takes into account and one can see that Ref. [6] takes fullest account of the statistical characteristics of resonance parameters and of the causes of resonance omission. However, one should bear in mind that the standard to which these characteristics are taken into account may vary. Thus, factor 4 is incorporated more accurately in Ref. [4] than in Ref. [6].

Comparison of the results obtained using these methods and the level to which factors determining the reliability of the evaluation have been taken into account should provide a firmer basis for the evaluation of mean parameters. The use of the methods described to evaluate the mean parameters for ^{235}U on the basis of the data provided in Ref. [3] in which resonances are subdivided according to spin tends to support this conclusion. The statistical data can be used to make an evaluation based on the total set of resonances and sets of resonances divided according to spin, and these results can be checked subsequently to see if they correlate. This also helps improve the reliability of the final evaluation. In order to improve the reliability

of evaluations the methods described were also used over various energy intervals. If results tallied over several intervals this was taken as proof that resonance omission was being taken into account adequately.

Use of the Δ_3 -statistics method [2] revealed that the set of 3^- -resonances obeys the condition of linearity for the rising sum of levels in the 0-100 eV region, and the set of 4^- -resonances and the total set of resonances obey that condition in the 0-73 eV interval. The mean values for $\langle D \rangle_0$ obtained using the method employed in Ref. [2] are given in Table 2 together with the relevant statistical errors for the 0-73 eV interval.

Linearity of the rising sum of levels is often looked upon as an indicator that there is no level omission. In fact, it only shows that the proportion of omitted levels is not dependent on energy, as demonstrated in the case of ^{238}U .

The results for $\langle D \rangle_0$ calculated using the method employed in Ref. [3] showed that $D_3^0(\alpha)$ and $D_4^0(\alpha)$ are practically independent of the parameter α over a wide range of its use. There are significant divergences from the plateau on the $D_3^0(\alpha)$ value in the 0-100 and 0-80 eV energy intervals; $D_3^0(\alpha)$ varies in the range 0.86-1.00 eV when $\alpha = 0.1-0.3$. Clearly, the dependence of D_3^0 on the determination interval and the parameter α is essentially related to the divergence of the experimental neutron width distribution for 3^- -resonances from the Porter-Thomas distribution in the region of the conditional threshold $\alpha < g\Gamma_n^0 \rangle_{3^-}$ (over 70 eV). The values given in Table 1 are for the 0-80 eV interval. The parameter $\langle D \rangle_0$ lies within the range 0.43-0.46 eV for change region of $\alpha \in [0.1-0.3]$; $\langle D \rangle_4$ lies on average within the range 0.79-0.84 eV. The error levels in the evaluation of $\langle D \rangle_0$ using the method employed in Ref. [3] includes statistical error ($0.52/\sqrt{N}$), error related to fluctuation in the mean values over energy intervals, and error related to the parameter α . The results of an evaluation of the mean values of $\langle g\Gamma_n^0 \rangle$ and $\langle D \rangle_0$ for ^{235}U using the method employed in Ref. [4] are given in Table 2.

The region of permissible change for the threshold height was limited to 80% of the part of the sample above the threshold, which is the usability condition for the statistical error evaluations in the method. The evaluated mean parameters (set of resonances not divided according to spin) turned out to be practically independent of t (see Fig. 1). The width cut-off threshold took the following form:

$$n(E) = (4.2 \cdot 10^{-8} E^{1.038} + 3.16 \cdot 10^{-6})t$$

Use of the method employed in Ref. [6] showed that the parameters $\langle g\Gamma_n^0 \rangle$ and $\langle D \rangle_0$ for 4^- -resonances in the 0-90 and 0-100 eV intervals are noticeably lower (by 9%) than for the 0-60, 0-70 and 0-80 eV intervals; this produces a divergence in the values obtained for $\langle D \rangle_0$ using the total set of parameters and those obtained using the sets for 3^- - and 4^- -resonances. This lends support to the view that level omission is not being taken into account accurately enough in the 80-100 eV region. This inaccuracy may be related to the choice of energy dependence parameters in the expression for the density of observable resonances ρ_0 in the method employed in Ref. [6]. A more realistic way of evaluating the coefficients incorporated in the expression for ρ_0 is to determine them in the area of linearity $N(E)$. Then the values which may be obtained for $\langle D \rangle_4^-$ and $\langle g\Gamma_n^0 \rangle_4$ tally with the results over narrower intervals and can be used to evaluate mean values (Fig. 2). In the 0-60 eV interval, the values of $\langle g\Gamma_n^0 \rangle$ for the total set of parameters and the set for 4^- -resonances are noticeably higher (by 8%) than for the 0-70, 0-80 and 0-90 eV intervals; this may be related to the small size of the sample.

The inaccuracy levels given for the mean values of $\langle g\Gamma_n^0 \rangle$ and $\langle D \rangle_0$ obtained using the method employed in Ref. [6] include statistical error and error due to fluctuation of the parameters over intervals. The value of $\langle D \rangle_0 = 0.426 \pm 0.016$ eV obtained using the total set of parameters tallies with the value obtained using the sets for 3^- - and 4^- -resonances. From Table 1, one can see that the values for $\langle D \rangle_0$ obtained using the method

employed in Ref. [4] are systematically higher than the values obtained using the method employed in Ref. [6]. This is due to the fact that the former method does not take into account level omission due to multiplicity.

To evaluate the mean parameters for ^{239}Pu , we used the evaluated data in Ref. [8]. In the energy region up to 500 eV, ^{239}Pu has 203 resonances. It was assumed that they are all of the s-type. The results of mean parameter calculations using the method employed in Refs [4, 6] are shown in Fig. 3.

Application of the Coceva method to the data from Ref. [8] revealed a clear dependence of mean values on the width of the interval over which averaging was being performed; this is due to the small size of the sample in the 0-350, 0-400, 0-450 eV intervals. In each interval we managed to ensure that the result was not dependent on the height of the conditional threshold for registration of the parameter t (see Fig. 3a). The latter is evidence that dependence on the energy interval is a characteristic of the data in Ref. [9] themselves and not of the way the method employed in Ref. [4] was being applied. In the 0-500 eV interval, $\langle g\Gamma_n^0 \rangle = (2.51 \pm 0.15) \cdot 10^{-4}$ eV; $\langle D \rangle_0 = (2.17 \pm 0.04)$ eV; $\langle S \rangle_0 = (1.16 \pm 0.05) \cdot 10^{-4}$. Use of the Fröhner method [6] also revealed a dependence of the values of $\langle g\Gamma_n^0 \rangle$ on the averaging interval in the 350-500 eV region and a plateau in the 270-330 eV region, (see Fig. 3b).

In the 0-500 eV region the mean values for $\langle g\Gamma_n^0 \rangle = (2.51 \pm 0.10) \cdot 10^{-4}$ eV and $\langle D \rangle_0 = (2.17 \pm 0.04)$ eV tally with the values obtained using the method employed in Ref. [4]. In our evaluation [8], the following mean parameter values were obtained for ^{239}Pu :

$\langle D \rangle_0 = 2.38 \pm 0.06$ eV, $\langle S_0 \rangle = (1.19 \pm 0.17) \cdot 10^{-4}$. The application of methods which allow for the introduction of a correction for level omission yielded a 10% reduction in the value of $\langle D \rangle_0$.

The evaluated resonance parameters for ^{247}Pu [10] were analysed. The mean parameter values obtained using the method employed in Ref. [4] were as follows: in the 0-1 keV interval, $\langle D \rangle_0 = 13.1 \pm 0.4$ eV,

$\langle g\Gamma_n^0 \rangle = (1.40 \pm 0.05) \cdot 10^{-3}$ eV (total number of resonances - 75, registered - 70);
 in the 0-0.9 keV interval, $\langle D \rangle_0 = 13.5 \pm 0.5$ eV, $\langle g\Gamma_n^0 \rangle = (1.38 \pm 0.05) \cdot 10^{-3}$ eV
 (total number of resonances - 67, registered - 62); in the 0-0.8 keV interval,
 $\langle D \rangle_0 = 13.5 \pm 0.5$ eV, $\langle g\Gamma_n^0 \rangle = (1.30 \pm 0.10) \cdot 10^{-3}$ eV (total number of
 resonances - 59, registered - 56). The method employed in Ref. [6], when applied
 to the data from Ref. [10], yielded the following mean parameter values: in the
 0-0.95 keV interval, $\langle D \rangle_0 = 13.1 \pm 0.3$ eV, $\langle g\Gamma_n^0 \rangle = (1.33 \pm 0.06) \cdot 10^{-3}$ eV
 (total number of resonances - 73, registered - 66); in the 0-0.85 keV interval,
 $\langle D \rangle_0 = 13.1 \pm 0.3$ eV, $\langle g\Gamma_n^0 \rangle = (1.28 \pm 0.06) \cdot 10^{-3}$ eV (six resonances omitted);
 in the 0-0.75 keV interval, $\langle D \rangle_0 = 13.0 \pm 0.3$ eV, $\langle g\Gamma_n^0 \rangle = (1.26 \pm 0.07) \cdot 10^{-3}$ eV
 (six resonances omitted).

The recommended mean parameter values for ^{240}Pu are as follows:
 $\langle D \rangle_0 = 13.1 \pm 0.03$ eV, $\langle g\Gamma_n^0 \rangle = (1.33 \pm 0.06) \cdot 10^{-3}$ eV, $\langle S_0 \rangle = (1.01 \pm 0.05) \cdot 10^{-4}$.
 In our evaluation [10] we obtained the following values: $\langle D \rangle_0 = 13.5 \pm 0.05$ eV;
 $\langle S_0 \rangle = (1.10 \pm 0.16) \cdot 10^{-4}$. Introduction of the correction for level omission
 produced a 3% drop in the value of $\langle D \rangle$.

The data from Ref. [9] and the data from the Japanese library [11] were
 used to evaluate ^{241}Pu . Their low quality makes analysis of these
 experimental data something of a problem. The difference in the resonance
 parameters relates to their neutron width distribution (Figs 4(a) and (b)),
 while the curves for the rising sum of resonances are practically identical
 (Fig. 5). Since the overall shape of the curve is not straight it could not be
 described using the approximations in the Fröhner method [6]; consequently,
 that method could not be used.

Application of the Coceva method [4] to the data from Ref. [9] revealed
 a noticeable dependence of evaluable mean parameter values on the energy
 interval used (Fig. 6(a)). In the 0-50 eV interval, $\langle D \rangle_0 = (1.06 \pm 0.06)$ eV,
 $\langle g\Gamma_n^0 \rangle = (1.55 \pm 0.15) \cdot 10^{-4}$ eV (five resonances omitted); in the 0-100 eV
 interval, $\langle g\Gamma_n^0 \rangle = (1.54 \pm 0.15) \cdot 10^{-4}$ eV, $\langle D \rangle_0 = (1.12 \pm 0.06)$ eV
 (13 resonances omitted).

The evaluated data in Ref. [11] in the resolved resonance region were obtained using experimental data on the capture cross-section [12] because these were preferable to the evaluation given in Ref. [9]. Use of the Coceva method [4] to analyse the data from Ref. [11] yielded a lower dependence of mean parameter values on the energy interval used by comparison with Ref. [9], particularly for $\langle D \rangle_0$ (Fig. 6(b)): In the 0-50 eV interval, $\langle g\Gamma_n^0 \rangle = (1.30 \pm 0.10) \cdot 10^{-4}$ eV, $\langle D \rangle_0 = (1.00 \pm 0.09)$ eV; in the 0-100 eV interval, $\langle g\Gamma_n^0 \rangle = (1.42 \pm 0.10) \cdot 10^{-4}$ eV, $\langle D \rangle_0 = (1.07 \pm 0.05)$ eV. The following mean parameter values may be recommended: $\langle D \rangle_0 = 1.07 \pm 0.07$ eV, $\langle g\Gamma_n^0 \rangle = (1.42 \pm 0.10) \cdot 10^{-4}$ eV, $\langle S_0 \rangle = 1.32 \pm 0.15) \cdot 10^{-4}$. When a correction for level suppression was introduced, the value of $\langle D \rangle_0$ fell by 25% by comparison with our evaluation [9] in which $\langle D \rangle_0$ was taken to be equal to 1.34 eV. The poor quality of available experimental data in the resolved resonance region for ^{241}Pu makes a reliable evaluation of resonance parameters impossible.

The upper boundary of the resolved resonance region for ^{242}Pu is 1 keV. Measurements in a higher energy region cannot be used for resonance analysis. The evaluated data from Ref. [13] were used to evaluate mean parameters for ^{242}Pu . The rise in the total number of levels is linear up to 1 keV. Application of the method employed in Ref. [4] to our data [13] yields values of $\langle D \rangle_0 = 15.0 \pm 2.0$ eV and $\langle g\Gamma_n^0 \rangle = (1.41 \pm 0.20) \cdot 10^{-3}$ eV for the 0-1 keV region. There is a strong dependence of mean parameter values on the width of the energy region over which averaging is being carried out, and on the registration threshold parameter. Analysis of the data from Ref. [13] using the method employed in Ref. [6] yields the following parameter values: $\langle D \rangle_0 = 13.5 \pm 0.5$ eV, $\langle g\Gamma_n^0 \rangle = (1.13 \pm 0.05) \cdot 10^{-3}$ eV in the 0-1 keV region (four resonances omitted); $\langle D \rangle_0 = 13.5 \pm 0.5$ eV, $\langle g\Gamma_n^0 \rangle = (1.17 \pm 0.06) \cdot 10^{-3}$ eV in the 0-0.85 keV region (three resonances omitted); $\langle D \rangle_0 = 13.4 \pm 0.5$ eV, $\langle g\Gamma_n^0 \rangle = (1.13 \pm 0.06) \cdot 10^{-3}$ eV in the 0-0.75 keV region (three resonances omitted); $\langle D \rangle_0 = 13.08 \pm 0.5$ eV, $\langle g\Gamma_n^0 \rangle = (1.10 \pm 0.06) \cdot 10^{-3}$ eV in the 0.65 keV region

(two resonances omitted). The recommended parameter values for ^{242}Pu are as follows: $\langle D \rangle_0 = 13.5 \pm 0.5$ eV, $\langle g\Gamma_n^0 \rangle = (1.13 \pm 0.05) \cdot 10^{-3}$ eV, $\langle S_0 \rangle = (0.84 \pm 0.05) \cdot 10^{-4}$. When a correction for level omission was introduced the value of $\langle D \rangle_0$ of 5% by comparison with our evaluation [13] in which we obtained values of $\langle D \rangle_0 = 14.23 \pm 0.5$ eV and $\langle g\Gamma_n^0 \rangle = (0.91 \pm 0.15) \cdot 10^{-4}$.

The most detailed measurements of the resonance parameters of ^{241}Am are in Ref. [14] which uses transmission measurements to obtain values for $2g\Gamma_n$ for all observable resonances in the 1-150 eV region and values for $\Gamma\gamma$ for 40% of resonances. Use of the Coceva method [4] to analyse the data in Ref. [14] produced the following mean parameter values: in the 0-50 eV region, $\langle D \rangle_0 = 0.552 \pm 0.050$ eV, $\langle g\Gamma_n^0 \rangle = (3.7 \pm 0.3) \cdot 10^{-5}$ eV (total number of resonances in the region - 89, 76 resonances registered, i.e. 15% level omission); in the 0-75 eV region, $\langle D \rangle_0 = 0.572 \pm 0.050$ eV, $\langle g\Gamma_n^0 \rangle = (4.3 \pm 0.7) \cdot 10^{-5}$ eV (total number of levels - 132, registered - 108); in the 0-100 eV region, $\langle D \rangle_0 = 0.570 \pm 0.050$ eV, $\langle g\Gamma_n^0 \rangle = (4.47 \pm 0.7) \cdot 10^{-5}$ eV (total number of levels - 171, registered - 136).

Use of the Fröhner method [6] to analyse data from Ref. [10] yields the following mean parameter values: in the 0-60 eV region, $\langle D \rangle_0 = 0.50 \pm 0.08$ eV, $\langle g\Gamma_n^0 \rangle = (3.5 \pm 0.8) \cdot 10^{-5}$ eV (total number of levels - 119, registered - 88); in the 0-80 eV region, $\langle D \rangle_0 = 0.62 \pm 0.07$ eV, $\langle g\Gamma_n^0 \rangle = (4.9 \pm 0.6) \cdot 10^{-5}$ eV.

From the above one may draw the following conclusions:

1. Evaluated values have been obtained for the mean parameters for ^{235}U . There is a high level of agreement between the evaluations of mean data for the total set and for the set divided according to spin;
2. Spin identification of the observable resonances from the set of data on ^{235}U enhances the reliability of the evaluation since one can then also check for agreement of results with respect to the total set of data and the set divided according to spin;

3. Evaluated values have been obtained for the mean parameters for ^{239}Pu , ^{240}Pu , ^{242}Pu and ^{241}Am using the methods employed in Refs [4, 6]. In view of the low quality and contradictory nature of the data on ^{241}Pu , new measurements of the total cross-section and the fission cross-section should be carried out for this nucleus using the type experiment employed in Ref. [14] for the 0-100 eV resolved resonance region.

REFERENCES

- [1] KON'SHIN, V.A., SALYAKHOV, N.K., Evaluation of mean parameters using data from the resolved resonance region for ^{238}U , Vopr.At.Nauki i Tekhniki, Ser.Yad.Konstanty 4 (1985) 3 [in Russian].
- [2] DYSON, F.T., MEHTA, M.L., Statistical theory of the energy levels of complex systems, J. Math. Phys. 4 (1963) 701-719.
- [3] MOORE, M.S., MOSES, I.D., KEYWORTH, G.A., et al., Spin determination of resonance structure in ($^{235}\text{U} + n$) below 25 keV, Phys. Rev. C18 (1978) 1328-1348.
- [4] COCEVA, C., STEFANON, M., Experimental aspects of the statistical theory of nuclear spectra fluctuations, Nucl. Phys. 315 (1979) 1-20.
- [5] DELFINI, G., GRUPPELAAR, H., "Maximum likelihood analysis of resolved resonance parameters for some fission product nuclides", Neutron cross-sections of fission product nuclei (Proc. of the specialists meeting, Bologna, Italy, 1979, Regione Technica Interna), (1979) 169-178.
- [6] FROHNER, F.H., "Level density estimation with account of unrecognized multiplets applied to uranium and plutonium resonance data", Proc. of the IAEA consultants meeting on uranium and plutonium isotope resonance parameters, Vienna, 1981, IAEA, Vienna (1981) 103-111.
- [7] FROHNER, F.H., "Statistical inference of level densities from resolved resonance parameters", Proc. of the IAEA advisory group meeting on basis and applied problems of nuclear level densities, Brookhaven, 1983, Brookhaven (1983) 219-244.
- [8] ANTSIPOV, G.V., BAKHANOVICH, L.A., KON'SHIN, V.A., et al., Evaluation of nuclear data for ^{239}Pu , Preprint Nos 12-16, ITMO AN BSSR [Institute of Heat and Mass-exchange of the Byelorussian SSR Academy of Sciences], Minsk (1981) [in Russian].
- [9] KON'SHIN, V.A., ANTSIPOV, G.V., SUKHOVITSKIJ, E.Sh., Evaluation of nuclear data for ^{241}Pu in the 10^{-3} eV-15 MeV neutron energy region, Preprint No. 3, ITMO AN BSSR, Minsk (1979) [in Russian].
- [10] ANTSIPOV, G.V., KON'SHIN, V.A., SUKHOVITSKIJ, E.Sh., Nuclear constants for plutonium isotopes, Nauka i tekhnika, Minsk (1982) [in Russian].

- [11] KIKUCHI, Y., SEKINE, N., Evaluation of neutron nuclear data of ^{241}Pu for JENDL-2, JAERI-M-84-111 (1984).
- [12] WESTON, L.W., TODD, J.H., Multilevel resonance parameters of plutonium-241, Nucl. Sci. and Engng. 68 (1978) 125.
- [13] ANTSIPOV, G.V., BAKHANOVICH, L.A., KON'SHIN, V.A., "Evaluation of nuclear data for ^{242}Pu in the resolved and unresolved region (10^{-5} eV-200 keV)", Scientific publications of the ITMO AN BSSR, Minsk (1979) 3-52 [in Russian].
- [14] DERRIEN, H., LUCAS, B., "The total cross-section and the fission cross-section of ^{241}Am in the resonance region, resonance parameters", Nucl. cross-sections and technol. (Proc. Conf. 3-7 March, Washington, 1975, Vol. 2), NBS Special publ. 425 (1975) 637.

Submitted for publication 17 March 1986

Table 1

Inclusion of factors affecting the reliability of mean resonance parameter evaluations in the various methods.

Methods	Factors					
	1	2	3	4	5	6
[2]			-	+	-	-
[3]	-	-	-	-	+	-
[4]	+	-	-	+	+	-
[6]	+	+	+	+	+	+

Table 2

Results of an evaluation of the parameters $\langle g\Gamma_n^0 \rangle$, $\langle D \rangle_0$ and $\langle S_0 \rangle$ for ^{235}U , obtained by analysing the experimental data from Ref. [3] using various methods.

Parameter	Type of parameter set	Method				Final evaluation
		[2]	[3]	[4]	[6]	
$\langle g\Gamma_n^0 \rangle, 10^{-5}$ eV	3 ⁻ resonances	-	-	3,56 \pm 0,54	3,30 \pm 0,51	3,30 \pm 0,51
	4 ⁻ resonances	-	-	4,23 \pm 0,56	4,50 \pm 0,58	4,50 \pm 0,58
	Total set	-	-	3,93 \pm 0,38	4,07 \pm 0,40	4,07 \pm 0,40
$\langle D \rangle_0$, eV	3 ⁻ resonances	1,090 \pm 0,060	0,982 \pm 0,127	1,019 \pm 0,037	0,926 \pm 0,050	0,926 \pm 0,050
	4 ⁻ resonances	0,905 \pm 0,053	0,820 \pm 0,088	0,801 \pm 0,027	0,790 \pm 0,040	0,790 \pm 0,040
	Total set	0,491 \pm 0,035	0,447 \pm 0,036	0,448 \pm 0,011	0,434 \pm 0,016	0,426 \pm 0,016
$\langle S_0 \rangle, 10^{-4}$	3 ⁻ resonances	-	-	0,80 \pm 0,11	0,815 \pm 0,11	0,815 \pm 0,11
	4 ⁻ resonances	-	-	0,94 \pm 0,12	1,01 \pm 0,12	1,01 \pm 0,12
	Total set	-	-	0,88 \pm 0,09	0,94 \pm 0,09	0,95 \pm 0,09

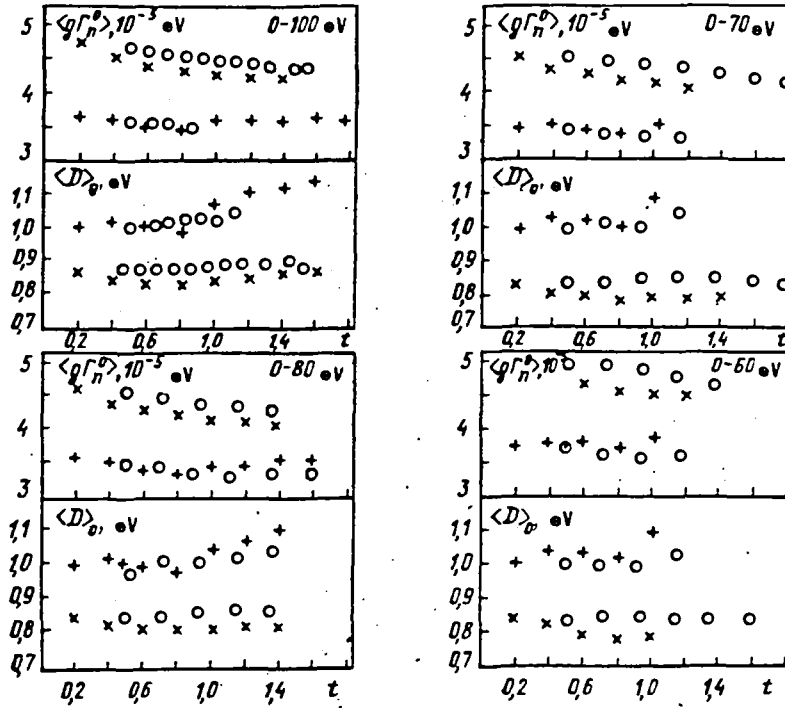


Fig. 1.

Calculated results for the mean values of $\langle D \rangle_0$ and $\langle g\Gamma_n^0 \rangle$ using the method employed in Ref. [4] for ^{235}U , based on the data in Ref. [3] for various energy intervals. Expression (2) is used to set the threshold; x, + - threshold parameters for $A = 4.2 \cdot 10^{-8}$, $B = 1.038$, $C = 3.16 \cdot 10^{-6}$; o - as before, except $C = 3.16 \cdot 10^{-7}$ (+, o - 3-resonances; x, o - 4-resonances).

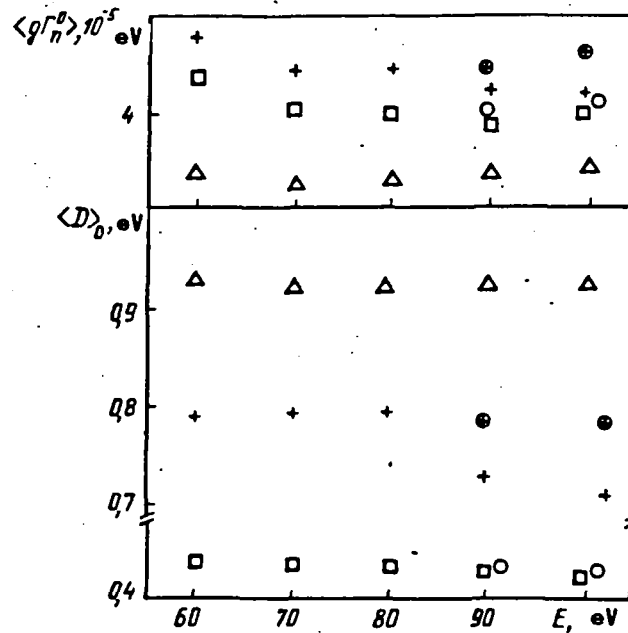


Fig. 2.

Calculated results for the mean resonance parameters for ^{235}U for various energy intervals using the method employed in Ref. [6]. Set of resonances with spin: Δ - $J = 3$; + - $J = 4$; \oplus - corrected results for the set $J = 4$; \square - set of resonances not divided according to spin; o - the same for corrected results.

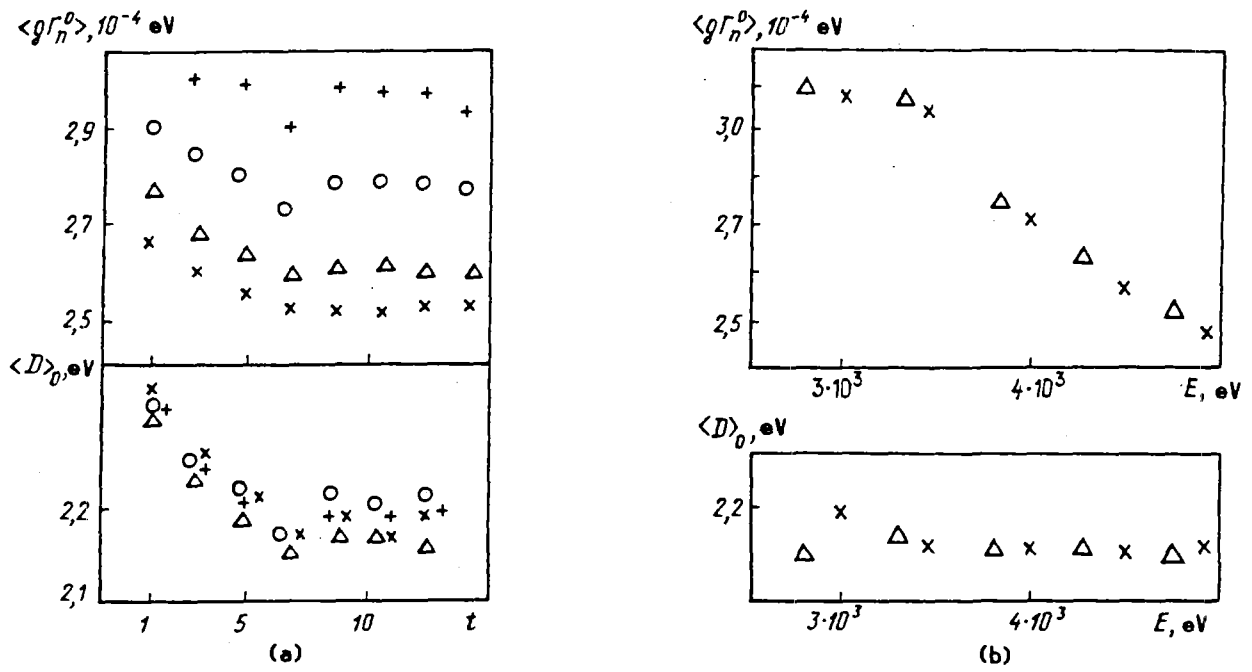


Fig. 3. Results obtained by applying the method employed in Refs. [4] (a) and [6] (b) to a set of ^{239}Pu resonance parameters based on data from Ref. [9] for the intervals: 0-500 eV (x), 0-450 eV (Δ), 0-400 eV (a), 0-350 eV (+).

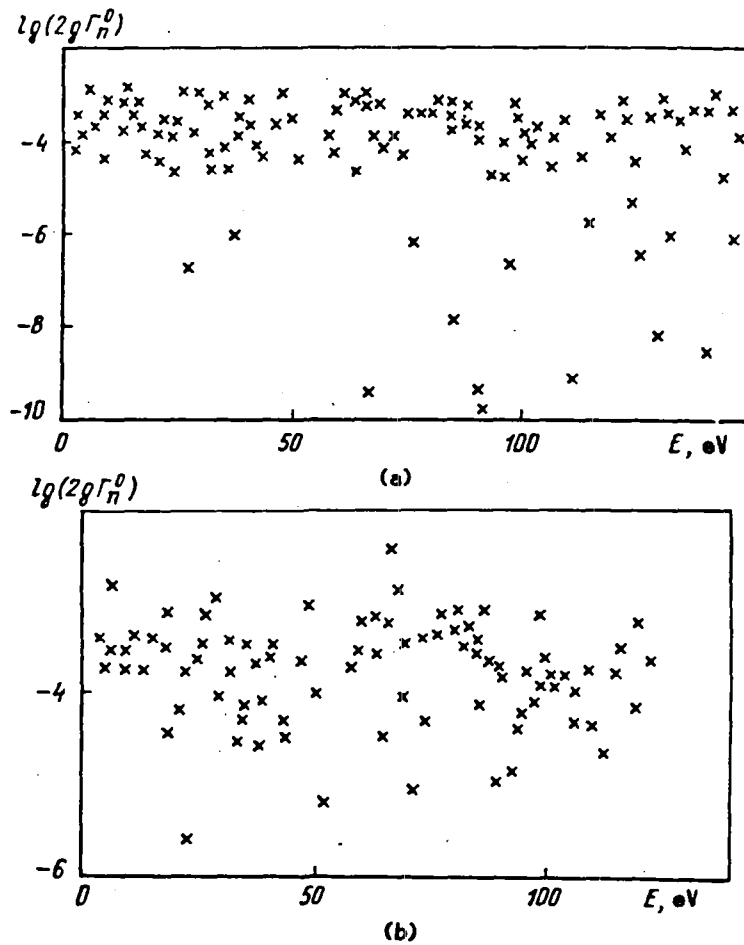


Fig. 4. Reduced neutron widths for ^{241}Pu resonances based on data from Refs. [9] (a) and [11] (b).

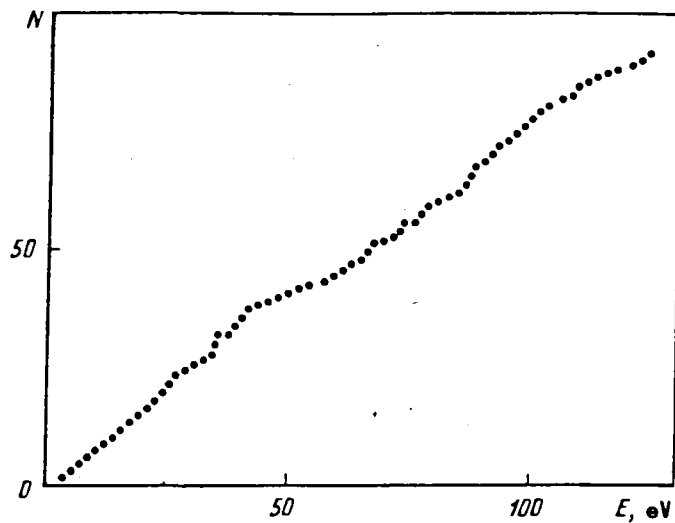


Fig. 5. Rising sums of resonances for ^{241}Pu based on data from Ref. [9] and [11] (the curves coincide).

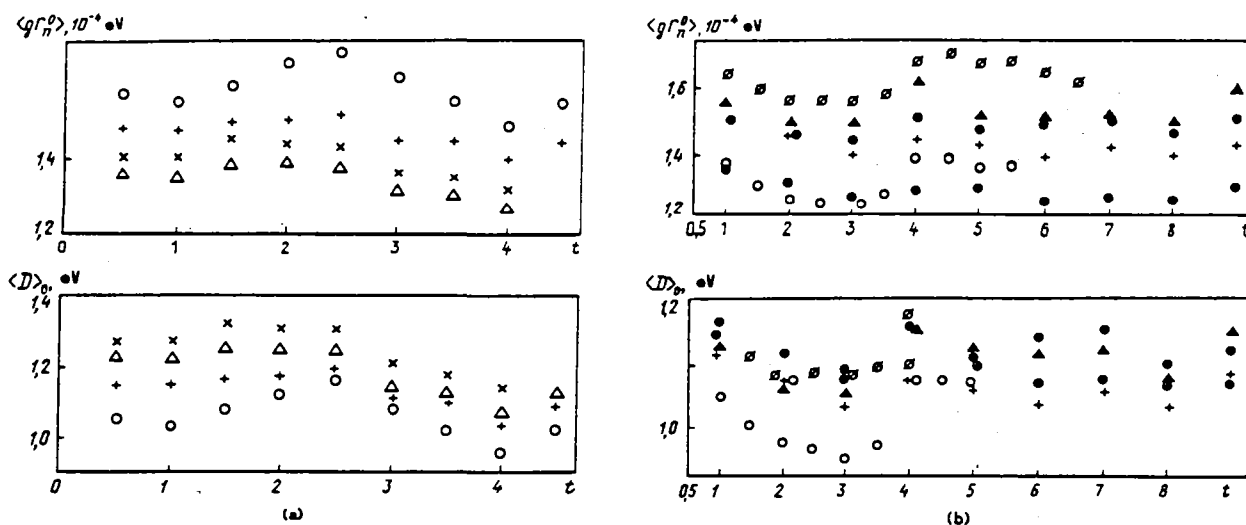


Fig. 6. Results obtained by applying the Coceva method [4] to ^{241}Pu resonance parameters based on evaluated data from Refs. [9] (a) and [11] (b) for the intervals 0-150 eV (x), 0-140 eV (Δ), 0-125 eV (⊕), 0-100 eV (+), 0-80 eV (e), 0-70 eV (Δ), 0-60 eV (∅), 0-50 eV (o).